

Development of the High-Pressure Direct-Injected, Ultra Low-NO_x Natural Gas Engine

Final Report

V.K. Duggal, E.J. Lyford-Pike, and J.F. Wright
Cummins, Inc.
Columbus, Indiana, USA

M. Dunn, D. Goudie, and S. Munshi
Westport Innovations, Inc.
Vancouver, British Columbia, Canada



NREL

National Renewable Energy Laboratory
1617 Cole Boulevard, Golden, Colorado 80401-3393
303-275-3000 • www.nrel.gov

Operated for the U.S. Department of Energy
Office of Energy Efficiency and Renewable Energy
by Midwest Research Institute • Battelle

Development of the High-Pressure Direct-Injected, Ultra Low-NO_x Natural Gas Engine

Final Report

V.K. Duggal, E.J. Lyford-Pike, and J.F. Wright
Cummins, Inc.
Columbus, Indiana, USA

M. Dunn, D. Goudie, and S. Munshi
Westport Innovations, Inc.
Vancouver, British Columbia, Canada

NREL Technical Monitor: M. Frailey

Prepared under Subcontract No. NCI-1-31036-01



NREL

National Renewable Energy Laboratory
1617 Cole Boulevard, Golden, Colorado 80401-3393
303-275-3000 • www.nrel.gov

Operated for the U.S. Department of Energy
Office of Energy Efficiency and Renewable Energy
by Midwest Research Institute • Battelle

NOTICE

This report was prepared as an account of work sponsored by an agency of the United States government. Neither the United States government nor any agency thereof, nor any of their employees, makes any warranty, express or implied, or assumes any legal liability or responsibility for the accuracy, completeness, or usefulness of any information, apparatus, product, or process disclosed, or represents that its use would not infringe privately owned rights. Reference herein to any specific commercial product, process, or service by trade name, trademark, manufacturer, or otherwise does not necessarily constitute or imply its endorsement, recommendation, or favoring by the United States government or any agency thereof. The views and opinions of authors expressed herein do not necessarily state or reflect those of the United States government or any agency thereof.

Available electronically at <http://www.osti.gov/bridge>

Available for a processing fee to U.S. Department of Energy and its contractors, in paper, from:

U.S. Department of Energy
Office of Scientific and Technical Information
P.O. Box 62
Oak Ridge, TN 37831-0062
phone: 865.576.8401
fax: 865.576.5728
email: <mailto:reports@adonis.osti.gov>

Available for sale to the public, in paper, from:

U.S. Department of Commerce
National Technical Information Service
5285 Port Royal Road
Springfield, VA 22161
phone: 800.553.6847
fax: 703.605.6900
email: orders@ntis.fedworld.gov
online ordering: <http://www.ntis.gov/ordering.htm>



Printed on paper containing at least 50% wastepaper, including 20% postconsumer waste

Table of Contents

List of Figures	ii
List of Tables	iv
List of Acronyms and Abbreviations	v
1.0 Executive Summary	1
2.0 Introduction	2
2.1 Project Objectives	3
3.0 Engine Development and Evaluation	4
3.1 Engine and Test Cell	4
3.2 Modeling and Analysis	6
3.2.1 Objective	6
3.2.2 Accomplishment Summary	7
3.2.3 Accomplishment Details	7
3.3 Diesel Baseline Testing	19
3.3.1 Objective	19
3.3.2 Accomplishment Summary	20
3.3.3 Accomplishment Details	20
3.4 HPDI Baseline Testing	22
3.4.1 Objective	22
3.4.2 Accomplishment Summary	22
3.4.3 Accomplishment Details	22
3.5 Preliminary Optimization: EGR Rate, Injection Timing, Fuel Pressure	26
3.5.1 Objective	26
3.5.2 Accomplishment Summary	26
3.5.3 Accomplishment Details	26
3.6 Oxidation Catalyst Testing	32
3.6.1 Objective	32
3.6.2 Accomplishment Summary	33
3.6.3 Accomplishment Details	33
3.7 Hardware and Controls Improvement	37
3.7.1 Objective	37
3.7.2 Accomplishment Summary	38
3.7.3 Accomplishment Details	38
3.8 Optimization and Calibration Refinement	45
3.8.1 Objective	45
3.8.2 Accomplishment Summary	45
3.8.3 Accomplishment Details	46
3.9 Transient Testing	58
3.9.1 Objective	58
3.9.2 Accomplishment Summary	58
3.9.3 Accomplishment Details	58
4.0 Conclusions and Recommendations	60
5.0 References	61

List of Figures

Figure 1: ISX Engine.....	4
Figure 2: High-Pressure EGR Loop Schematic.....	4
Figure 3: Test Cell with ISX Engine	5
Figure 4: CO ₂ Sampling Probes for Inlet Charge EGR Measurement	6
Figure 5: GT-Power Engine Simulation Model Layout for the ISX-EGR Engine with VGT	8
Figure 6: AVL 8-Mode Test Points and 450 Hp/1,650 ft-lb (335 Kw/2,236 N-m) Torque Curve .	9
Figure 7: NO _x Emissions Prediction Compared with Measurements for AVL Modes 3-8.....	10
Figure 8: Distribution of EGR Between Cylinders at AVL Modes 3, 5, and 8.....	11
Figure 9: Original and Modified Rate of Heat Release Profile at AVL Mode 8.....	11
Figure 10: Original and Smaller Compressor Speed Maps with AVL Mode 4 Operating Point ..	12
Figure 11: Original and Smaller Compressor Speed Maps with AVL Mode 8 Operating Point ..	12
Figure 12: Effect of Turbine Ring Gap (Rack Position) at AVL Mode 8 on EGR Rate and VGT Speed	13
Figure 13: Standard Hardware Compressor Speed Map and Operating Points at Various Turbine Ring Gaps (at AVL Mode 8).....	13
Figure 14: Effect of Turbine Ring Gap (Rack Position) on EGR Rate and Cylinder Peak Pressure with Smaller Compressor Trim (at AVL Mode 4)	14
Figure 15: Smaller Trim Compressor Speed Map and Operating Points at Various Turbine Ring Gaps (at AVL Mode 4).....	14
Figure 16: Effect of EGR Valve Diameter on Airflow Rate and EGR Rate at AVL Mode 8.....	15
Figure 17: Effect of VGT Turbine Size on EGR Rate and VGT Speed at AVL Mode 8	15
Figure 18: Effect of VGT Turbine Size on the Compressor Operating Point at AVL Mode 8.....	16
Figure 19: Effect of EGR Venturi Throat Diameter on EGR Rate and VGT Speed at AVL Mode 8	17
Figure 20: Effect of EGR Venturi Throat Diameter on IMEP and ISFC at AVL Mode 8.....	17
Figure 21: Impact of Injection Timing Retard on Fuel Efficiency Penalty	19
Figure 22: 0.5 g/bhp-hr NO _x Model of AVL Test Points on Smaller Trim Compressor Speed and Efficiency Maps	19
Figure 23: ESC 13-Mode Test Points and Torque Curve.....	21
Figure 24: Photograph of the IFSM Assembly.....	23
Figure 25: High-Pressure Diesel Fuel Pump	23
Figure 26: The J-31 HPDI Injector.....	24
Figure 27: Installed J-31 Injectors and Wiring Harness	24
Figure 28: Injection Pulse and Timing Diagram	24
Figure 29: ESC Mode 5 and 10 EGR Swings	27
Figure 30: Pilot Fueling Swings—Coefficient of Variance (COV) of IMEP Response	29
Figure 31: Pilot Fueling Swings—Corrected BSNO _x Response	29
Figure 32: Pilot Fueling Swings—Brake Specific Carbon Monoxide (BSCO) Response	29
Figure 33: Pilot Fueling Swings—Brake Specific CH ₄ (BSCH ₄) Response	30
Figure 34: Pilot Fueling Swings—BSFC Response	30
Figure 35: AVL Mode 8 GRP Swings—BSFC and maximum cylinder pressure (Pmax).....	31
Figure 36: AVL Mode 8 GRP Swings—EMT and IMP	31
Figure 37: AVL Mode 8 GRP Swings—BSNO _x and BSNMHC	31
Figure 38: AVL Mode 8 GRP Swings—BSCH ₄ and BSCO.....	31
Figure 39: ESC Mode 10 GRP Swings—BSFC and Pmax.....	32
Figure 40: ESC Mode 10 GRP Swings—EMT and IMP	32
Figure 41: ESC Mode 10 GRP Swings—BSNO _x and BSNMHC.....	32
Figure 42: ESC Mode 10 GRP Swings—BSCH ₄ and BSCO.....	32
Figure 43: CO, NMHC, and CH ₄ Conversion Efficiencies of 40 g/ft ³ Catalyst.....	34
Figure 44: CO, NMHC, and CH ₄ Conversion Efficiencies of 80 g/ft ³ Catalyst.....	34
Figure 45: CO, NMHC, and CH ₄ Conversion Efficiencies of 160 g/ft ³ Catalyst.....	35

Figure 46: PM Modal Contribution Breakdown over AVL 8-Mode Test Cycle	36
Figure 47: Comparison of AVL Cycle-Weighted Emissions Before and After Oxidation Catalyst	37
Figure 48: Emissions Reduction Resulting from Oxidation Catalyst (Based on AVL Weighted Emissions; See Figure 47).....	37
Figure 49: New Engine Installed in Test Cell	39
Figure 50: New Engine with Westport Production-Intent Fuel System and Controls.....	39
Figure 51: Top View Schematic of Head Showing Cylinders, Intake Runners, and EGR Sample Locations	40
Figure 52: EGR Probe #1 in Intake Air Horn.....	40
Figure 53: Typical “Pepper Pot” Sample Probe Installed in Cylinder Head.....	41
Figure 54: EGR Sample Switching Manifold.....	41
Figure 55: EGR Sampling Probes after 50 Hours of Operation.....	42
Figure 56: Average EGR Fraction at Each Sample Location over Various Speed-Load Conditions; Red Dots Show Cylinder Location Relative to Sample Location (466 Samples Total)	43
Figure 57: Difference Between EGR Fraction Determined from Sample Locations and Average of Sample Locations 2-8.....	43
Figure 58: Second EGR Cooler Mounted in Series with Original Cooler	44
Figure 59: Second EGR Cooler.....	44
Figure 60: Cooled EGR Temperatures with and without the Extra EGR Cooler.....	45
Figure 61: Calibration Test Points under the 450 hp/1,650 ft-lb Torque Curve.....	47
Figure 62: Minimized BSNO _x vs. BSFC Tradeoff and Associated CH ₄ and CO at ESC Mode 2	48
Figure 63: Engine Settings for Minimized BSNO _x -BSFC Tradeoff Curve at ESC Mode 2	49
Figure 64: Contour Plots of BSNO _x RSM at ESC Mode 2 (Units: BSNO _x = g/bhp-hr, Fuel Pressure = bar, GSOI = degrees BTDC, VGT = mm).....	50
Figure 65: Contour Plots of BSFC RSM at ESC Mode 2 (Units: BSFC = g/bhp-hr, Fuel Pressure = bar, GSOI = degrees BTDC, VGT = mm)	50
Figure 66: Contour Plots of BSCH ₄ RSM at ESC Mode 2 (Units: BSCH ₄ = g/bhp-hr, Fuel Pressure = bar, GSOI = degrees BTDC, VGT = mm).....	50
Figure 67: Contour Plots of BSCO RSM at ESC Mode 2 (Units: BSCO = g/bhp-hr, Fuel Pressure = bar, GSOI = degrees BTDC, VGT = mm)	51
Figure 68: Minimized BSNO _x and BSCO vs. BSFC at Various GSOI Settings at ESC Mode 2..	51
Figure 69: Gas SOI Comparison—Manual vs. Automatic.....	52
Figure 70: Fuel Pressure Comparison—Manual vs. Automatic.....	52
Figure 71: VGT Ring Gap Comparison—Manual vs. Automatic.....	52
Figure 72: EGR Valve Position Comparison—Manual vs. Automatic.....	52
Figure 73: Equivalence Ratio Comparison—Manual vs. Automatic	53
Figure 74: Measured EGR Fraction Comparison—Manual vs. Automatic	53
Figure 75: Example of In-Cylinder Pressure Measurement	55
Figure 76: Example of Heat Release Rate from In-Cylinder Pressure Measurement	55
Figure 77: FTP Transient Speed and Load Profile.....	56
Figure 78: Target 450 hp (1,650 ft-lb/2,237 N-m) Torque Curve and Tested Torque Curve	56
Figure 79: Transient Calibration Development	57
Figure 80: Transient NO _x , EGR Valve, and EGR Fraction Response during Rapid Acceleration	58
Figure 81: Final Transient FTP Tests—BSNO _x vs. BSPM.....	59
Figure 82: Final Transient FTP Tests—BSNO _x vs. BSHC	59
Figure 83: Final FTP Tests—BSNO _x vs. BTE.....	60

List of Tables

Table 1: Summary of Potential Engine Modifications	18
Table 2: AVL 8-Mode Test Results under Diesel Fueling.....	20
Table 3: ESC 13-Mode Test Results under Diesel Fueling.....	21
Table 4: AVL 8-Mode Test Results under HPDI Fueling with Initial Calibration	25
Table 5: Summary of Pilot Fueling Swings	28
Table 6: ESC Mode 2—DoE Parameters and Ranges.....	48
Table 7: Final ESC 13-Mode Emissions Results.....	53
Table 8: Final AVL 8-Mode Emissions Results.....	54

List of Acronyms and Abbreviations

A/F	Air/fuel
ATDC	After top dead center
AVL	Anstalt für Verbrennungskraftmaschinen (Institute for Internal Combustion Engines)
BSCH ₄	Brake specific methane
BSCO	Brake specific carbon monoxide
BSFC	Brake specific fuel consumption
BSHC	Brake specific hydrocarbons
BSNMHC	Brake specific nonmethane hydrocarbons
BSNO _x	Brake specific nitrogen oxides
BSPM	Brake specific particulate matter
BTDC	Before top dead center
BTE	Brake thermal efficiency
CA	Crank angle
CH ₄	Methane
CO	Carbon monoxide
CO ₂	Carbon dioxide
COV	Coefficient of variance
DoE	Design of experiments
ECM	Engine control module
EGR	Exhaust gas recirculation
EGT	Exhaust gas temperature
EMT	Exhaust manifold temperature
ESC	European Stationary Cycle
ft-lb	Foot-pounds
FTP	Federal Test Procedure
g/bhp-hr	Grams per brake horsepower hour
GRP	Gas rail pressure
GSOI	Gas start of injection
HC	Hydrocarbons
hp	Horsepower
HPDI	High Pressure Direct Injection
HRR	Heat release rate
Hz	Hertz
IDM	Intelligent driver module
IFSM	Integrated fuel supply module
IMEP	Indicated mean effective pressure
IMP	Intake manifold pressure
ISFC	Indicated specific fuel consumption
IVC	Intake valve closure
kW	Kilowatt
L	Liter
mm	Millimeter
MPa	Megapascals
ms	Millisecond
μs	Microsecond
NGNGV	Next Generation Natural Gas Vehicle

N-m	Newton-meter
NMHC	Nonmethane hydrocarbons
NO _x	Nitrogen oxides
NTE	Not-to-exceed
Pd	Palladium
P _{ivc}	Charge pressure at intake valve closure
PM	Particulate matter
P _{max}	Maximum cylinder pressure
ppm	Parts per million
PPW	Pilot pulse width
PSOI	Pilot start of injection
Pt	Platinum
PW	Pulse width
RIT	Relative injection timing (equivalent to pilot separation)
RSM	Response surface model
SOF	Soluble organic fraction
SOI	Start of injection
SOL	Solids
SV	Space velocity
TDC	Top dead center
TDM	Test Data Manager (by Schenck-Ricardo)
T _{ivc}	Charge temperature at intake valve closure
ULSD	Ultra-low sulfur diesel
VGT	Variable geometry turbocharger
VIP	Variable injection pressure

1.0 Executive Summary

Natural gas is a domestically available alternative fuel. The U.S. Department of Energy supports natural gas engine and vehicle research and development to help the United States reach its goal of reducing dependence on imported petroleum. Another benefit of natural gas vehicles is that they can reduce emissions of regulated pollutants compared with diesel vehicles. The U.S. Department of Energy supported the work described in this report through its Next Generation Natural Gas Vehicle activity, which is led by the National Renewable Energy Laboratory.

Current medium- and heavy-duty natural gas engines use lean-burn spark ignition technology to achieve low emissions with full-load efficiencies slightly lower than those of diesel engines. Part-load efficiencies, however, are much lower than those of diesel engines.

Westport Innovations Inc.'s High Pressure Direct Injection (HPDI™) natural gas fuel system used in an otherwise unmodified heavy-duty diesel engine reduces nitrogen oxides (NO_x) and particulate matter (PM) emissions while maintaining diesel-like efficiencies at full and part loads. The fuel system directly injects a small quantity of pilot diesel fuel that ignites directly injected high-pressure natural gas.

This project targeted development of a high-efficiency, low-emission natural gas engine for heavy-duty trucks. Specifically, it targeted the demonstration of a Cummins ISX engine using HPDI natural gas fueling and exhaust gas recirculation (EGR) meeting the following specifications:

- Peak torque of 1,650 ft-lb (2,236 N-m)
- Rated power of 450 hp (335 kW)
- Peak thermal efficiency of 40% with typical diesel part-load efficiency
- NO_x emissions of 0.5 g/bhp-hr
- PM emissions of 0.1 g/bhp-hr
- Substitution of diesel with natural gas greater than 90% over the certification cycle

Testing and modeling of an otherwise unmodified Cummins ISX engine with EGR and HPDI fueling indicated that the program goals could not be met with the standard production hardware. Therefore, a turbocharger using a smaller trim compressor and a second EGR cooler were fitted to the engine along with an oxidation catalyst.

Compared with HPDI fueling without a catalyst, the catalyst reduced the AVL 8-mode cycle weighted PM emissions by 34% from 0.04g/bhp-hr to 0.03g/bhp-hr. Nonmethane hydrocarbon (NMHC) emissions were reduced by 54% and carbon monoxide (CO) emissions by 96%.

A steady-state engine calibration was developed using design of experiment test techniques. Testing over the European Stationary Cycle (ESC) 13-mode cycle resulted in weighted NO_x emissions of 0.37 g/bhp-hr, NMHC emissions of 0.2 g/bhp-hr, methane

(CH₄) emissions of 2.08 g/bhp-hr, PM emissions of 0.04 g/bhp-hr, and a weighted thermal efficiency of 36.1% (diesel-equivalent fuel consumption of 173 g/bhp-hr). Peak thermal efficiency was 39.5%, and weighted diesel (pilot) use was 6% of total fuel consumption. At high-load conditions, the pilot quantity accounted for less than 5% of total fuel consumption.

The engine, in its final hardware configuration, was shipped to the Cummins Engine Company, and the transient testing and calibration refinement was conducted at Cummins' facilities. The calibration met the targeted power and torque requirements of 450 hp and 1,650 ft-lb. Average NO_x emissions of 0.6 g/bhp-hr were repeatedly demonstrated over the Federal Test Procedure (FTP) cycle, with a best result of 0.56 g/bhp-hr. Total hydrocarbon emissions were approximately 5 g/bhp-hr, and much of this was assumed to be CH₄. Average PM emissions remained relatively constant at around 0.03 g/bhp-hr, and the average brake thermal efficiency was 34.1%, which is comparable with state-of-the-art diesel engines.

2.0 Introduction

Congress enacted the Clean Air Act Amendments of 1990 in response to continuing concern about air pollution. The Act's provisions will force broad changes in fuels and vehicles. For example, clean diesel, reformulated gasoline, and alternative fuels are now receiving wide attention as industry tries to comply with the Act. Many ozone non-attainment areas are focusing on heavy-duty alternative fuel vehicles for their State and Federal Implementation Plans because these vehicles have the potential to greatly reduce particulate matter (PM) and nitrogen oxides (NO_x) emissions. Also, alternative fuels may be easier to introduce for fleet-based heavy-duty vehicles because these vehicles often use central refueling depots.

Many technologies must be developed further to take full advantage of the properties of alternative fuels and to enable their widespread use. These include technologies for emissions control, increased energy efficiency, fuel-specific engine optimization strategies, and engine and fuel system hardware. The goal is to develop technologies that will make alternative fuels commercially competitive with diesel in terms of energy efficiency, performance, durability, driveability, cold-start ability, safety, and range, while having an emissions benefit.

Natural gas is a domestically available alternative fuel. The U.S. Department of Energy supports natural gas engine and vehicle research and development to help the United States reach its goal of reducing dependence on imported petroleum, as outlined in the Energy Policy Act of 1992. Another benefit of natural gas vehicles is that they can reduce emissions of regulated pollutants compared with diesel vehicles. The U.S. Department of Energy supported the work described in this report through its Next Generation Natural Gas Vehicle (NGNGV) activity, which is led by the National Renewable Energy Laboratory.

One goal of the NGNGV activity is to develop advanced, commercially viable, medium- and heavy-duty natural gas engines and vehicles that will achieve the U.S. Environmental Protection Agency's 2007/2010 heavy-duty emission levels before 2007. Another goal is to develop production-intent natural gas engines that meet current emission levels and

can be deployed commercially in the near term to gain immediate petroleum displacement and emission reduction benefits. The NGNGV activity is also supported by the South Coast Air Quality Management District and the California Energy Commission.

Current state-of-the-art medium- and heavy-duty natural gas engines employ lean-burn spark-ignition technology to achieve significant emissions reductions while maintaining full-load efficiency marginally lower than diesel engines. Because most of these natural gas engines originated as diesel engines, most are turbocharged and inherently have high cylinder pressures and high power density capability. Lean-burn spark-ignition engine technology lends itself well to these engines. However, current state-of-the-art natural gas engines suffer large efficiency penalties at part load and lesser penalties at full load compared with their diesel counterparts. There are three main reasons for this efficiency penalty in lean-burn spark-ignited natural gas engines: a lower knock-limited compression ratio; the inability to operate at very lean air/fuel ratios at low loads; and, leading to the third reason, the need to use a throttle at part load to limit air flow. These factors greatly influence thermal efficiency and, thus, vehicle operating cost and range.

Westport Innovations Inc.'s High Pressure Direct Injection (HPDI) natural gas fuel system can be used in an otherwise unmodified heavy-duty diesel engine to reduce NO_x and PM emissions while maintaining diesel-like power and efficiency at full and part loads [1,2]. The fuel system directly injects a small quantity of pilot diesel fuel that ignites directly injected high-pressure natural gas. The fuels are directly injected into the cylinder using a single fuel injector with concentric needles and separate injection holes for each fuel.

Exhaust gas recirculation (EGR) reduces NO_x in heavy-duty diesel engines. However high EGR rates can lead to increased PM emissions. Because directly injected natural gas has a lower propensity to form PM emissions than does diesel fuel, it is a good candidate for use with EGR. This report presents some of the development work combining EGR with the Westport HPDI natural gas fuel system on a Cummins ISX heavy-duty diesel engine.

2.1 Project Objectives

This project targeted the development of a high-efficiency, high-performance natural gas engine for heavy-duty trucks that can meet very low NO_x emissions levels. Specifically, the project targeted the demonstration of a Cummins ISX engine using HPDI natural gas fueling and EGR meeting the following specifications:

- Peak torque of 1,650 ft-lb (2,236 N-m)
- Rated power of 450 hp (335 kW)
- Peak thermal efficiency of 40% with typical diesel part-load efficiency
- NO_x emissions of 0.5 g/bhp-hr
- PM emissions of 0.1 g/bhp-hr
- Substitution of diesel with natural gas greater than 90% over the certification cycle

3.0 Engine Development and Evaluation

3.1 Engine and Test Cell

Engine Description

The Cummins ISX (Figure 1) is a six-cylinder 15 L heavy-duty engine with a 17:1 compression ratio. The engine uses a high-pressure EGR loop (Figure 2) that includes a variable geometry turbocharger (VGT), EGR valve, and EGR cooler. Engines are commercially available with ratings of 400-565 hp. The engine used in this work was rated at 450 hp (335 kW) and 1,650 ft-lb (2,236 N-m).



Figure 1: ISX Engine

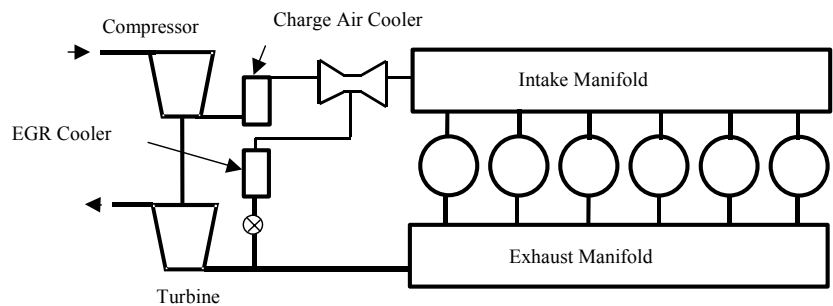


Figure 2: High-Pressure EGR Loop Schematic

The ISX engine with EGR was made commercially available in October 2002. This project began in 2001 before production engines were available, so initial work was conducted with a pre-production engine. A production ISX was used for later testing and final calibration. There were no fundamental hardware differences between these two engines, only changes to improve durability and robustness of controls. Therefore, the original modeling and test work using the pre-production engine was directly applicable to the production engine.

Test Cell Description

The test cell was fitted with equipment and services suitable for the ISX engine, including the following:

- AVL B-500 eddy current dynamometer with 480 kW capacity
- Meriam laminar flow element for air flow measurement
- Micro-Motion gas flow meter
- Gravimetric diesel fuel measurement system (pail and scale)
- Water-cooled charge air heat exchanger
- Water-cooled engine coolant heat exchanger
- Agilent Micro Gas Chromatograph for natural gas composition analysis
- AVL opacimeter
- Digalog data acquisition and controls system

An additional diesel fuel supply system was installed for ultra-low sulfur diesel (ULSD). This fuel has a sulfur content of less than 15 ppm to prevent the poisoning of exhaust catalysts. The ULSD will be used during future aftertreatment research.

The engine instrumentation included in-cylinder high-speed pressure transducers on all six cylinders. The transducers on cylinders 1 and 6 are flush-mounted to the fire deck and water cooled. Those on cylinders 2 through 5 are side mounted and separated from the combustion chamber by a drilled passage. Low-speed pressure and temperature sensors were installed at all necessary locations in the intake, charge air, EGR, and exhaust lines.

Emissions were measured with a Horiba 7500D-EGR exhaust gas analyzer. This system can monitor pre- or post-catalyst exhaust emissions and the carbon dioxide (CO₂) concentration in the engine intake manifold to determine EGR rates. PM is measured using a gravimetric method and a mini-dilution tunnel from Sierra Instruments. The engine and test cell are shown in Figure 3.



Figure 3: Test Cell with ISX Engine

Test Cell: Data Acquisition and Post-Processing

Three separate data streams are recorded in the test cell:

- General test cell instrumentation, using the Digalog system
- Engine parameter information, recorded from the engine control module (ECM)
- High-speed in-cylinder pressure measurements, using an AVL 619 Indiset

All data were typically collected at a 1-Hz sampling frequency, except for the in-cylinder pressure measurements, which were recorded at a 0.5-degree crank angle (CA) resolution. Probes at the entrance to the inlet manifold, to sample the CO₂ concentration

for calculation of the EGR rate, are shown in Figure 4. Later, when the engine was replaced, CO₂ samples were taken along the intake manifold near the intake valves. A Cummins electronic calibration tool records ECM data such as fueling and timing commands and EGR system control settings, which cannot be directly recorded by the main data acquisition system.



Figure 4: CO₂ Sampling Probes for Inlet Charge EGR Measurement

Data are typically recorded for 3 minutes. The test cell data and the ECM data are combined and processed using the software package Test Data Manager (TDM) by Schenck-Ricardo. TDM is an integrated data storage and processing tool that is secure and follows a quality assurance procedure to ensure that any changes are traceable. TDM cannot process high-speed data at present, so these are processed separately.

Test Cell: Validation

The engine was installed, broken-in and tested at Cummins Engine Company using a 565-hp calibration. The calibration was then changed to 450 hp, and an AVL 8-mode test was conducted. This same test was then performed at Westport to validate the Westport test cell. Comparison of these results showed that all instrumentation was functioning as required except for one intake manifold pressure sensor. This was replaced, and subsequent measurements were comparable to the Cummins measurements. Also, two test runs were conducted at Westport to check repeatability. As a result, the fuel mass measurement technique was modified to make the results more robust. With these few improvements, the test cell and engine were considered to be in good health. Data quality was monitored continuously during the test program.

3.2 Modeling and Analysis

3.2.1 Objective

Analyses of combustion and engine performance were conducted with the following objectives:

- Develop a model to help understand combustion processes and predict the effect of EGR on NO_x emissions and engine performance
- Anticipate the capability of the engine hardware to achieve the EGR levels needed to meet the targeted NO_x emissions
- Anticipate the engine settings required to meet the targeted NO_x level

The combustion/NO_x model and the engine performance model were validated using test data. The analytical tools will also be used during the engine testing phase to assist optimization.

3.2.2 Accomplishment Summary

An engine performance model was developed using GT-Power. The model was validated using test data with and without EGR under diesel and HPDI fueling. A combustion model (XPNO_x) for NO_x emissions was also developed at Westport. It is a multi-zone combustion model that calculates heat release rate and NO_x based on in-cylinder pressure traces. XPNO_x was validated using test cell data with and without EGR under diesel and HPDI fueling. Both were found to predict engine performance well with some limitations.

After validation, both models were used to predict the EGR rates, engine settings, and capability of the engine to meet the NO_x emissions target of 0.5 g/bhp-hr. Hardware deficiencies were identified, and suggestions for improvements were made. The suggested hardware changes included a smaller trim compressor and an extra EGR cooler. Using this new hardware, the models identified the likely engine settings to reach the 0.5 g/bhp-hr NO_x emissions target.

3.2.3 Accomplishment Details

GT Power: Engine Performance Model

GT-Power is a commercially available computer program that predicts engine performance. It can calculate performance data such as air flow rate, fuel flow rate, brake torque and power, brake mean effective pressure, intake manifold pressure, cylinder pressure versus CA, residual gas fraction, brake specific fuel consumption (BSFC), brake thermal efficiency (BTE), volumetric efficiency, heat release rate, mass burn profile, wall heat transfer, compressor/turbine work, and more. A GT-Power model of the six-cylinder Cummins ISX-EGR engine with a VGT was developed (Figure 5).

GT-Power: Engine Model Validation

Much of the steady-state engine testing was conducted over the AVL 8-mode test cycle, so the engine model was validated at these points (Figure 6). Modeling and validation were conducted with increasingly complex models:

- Diesel fuel only without EGR
- HPDI without EGR
- Diesel fuel only with EGR
- HPDI with EGR

This progression enabled successive validation of the base engine, EGR system, and HPDI fuel system models. The model was found to be a good predictor of actual engine performance at most conditions with some minor limitations. The model was not highly accurate at low fueling (idle) or conditions near the extremes of the turbocharger map.

With some limitation at low-power conditions, the model allows the prediction of the effects of major changes, such as changes to turbocharger characteristics, EGR rates, start of injection (SOI) timing, and so forth.

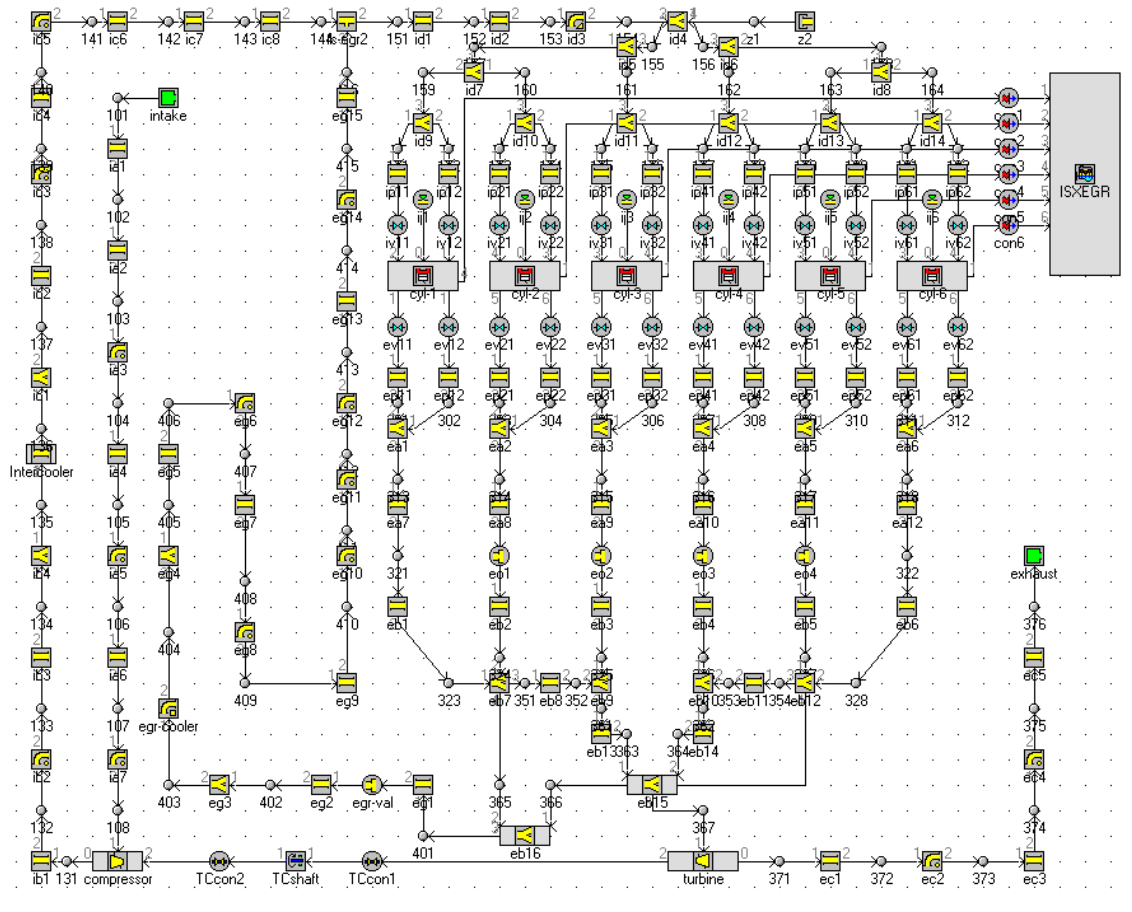


Figure 5: GT-Power Engine Simulation Model Layout for the ISX-EGR Engine with VGT

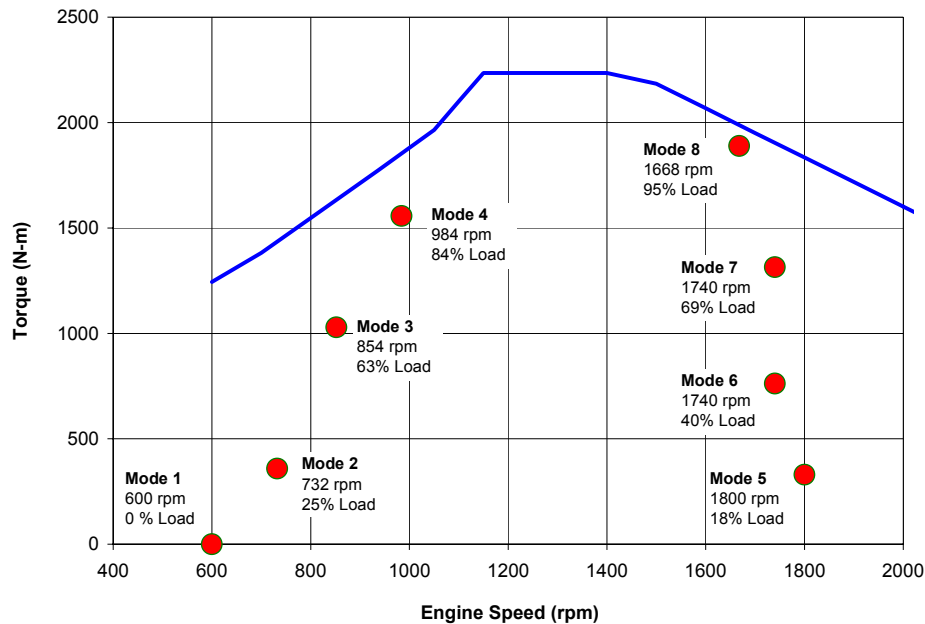


Figure 6: AVL 8-Mode Test Points and 450 Hp/1,650 ft-lb (335 Kw/2,236 N-m) Torque Curve

XPNOx: Combustion Model

XPNOx is computer program developed by Westport to estimate NO_x emissions. Based on actual cylinder pressure data from an engine test, it calculates the heat release rate, temperature, and resulting rate of NO production in each of many zones of burned gas.

Combustion in each gas packet is stoichiometric, with a separate combustion zone created for each CA degree. NO is generated according to the extended Zeldovich mechanism in each burned zone for a period of one “turbulent mixing time” after burning; after this, instantaneous mixing with unburned gas freezes the NO level. Experience with non-EGR ISX engines indicates that a turbulent mixing time of 0.6 ms characterizes NO formation over a wide range of conditions for both diesel and natural gas fueling. As the model evolved, a 0.3-ms mixing time was found to provide better predictions. After mixing, each burned-and-mixed zone expands to successively lower pressures and temperatures. The residual gas fraction is determined by satisfying mass and energy balances at inlet valve closure.

Calculated NO is sensitive to end-of-compression temperature, so the compression curve is corrected as necessary to have reasonable consistency with polytropic compression. A polytropic exponent is calculated from the variable-specific heat isentrope and a heat transfer estimate based on the Woschni correlation. Measured cylinder pressures are erratic at inlet valve closure, so end-of-compression temperature is best estimated by comparing measured and calculated polytropes at the upper end of the compression curve.

XPNO_x: Model Validation

XPNO_x was validated at common points on the AVL 8-mode or European Stationary Cycle (ESC) 13-mode tests, with diesel and HPDI fueling, both with and without EGR. Only the HPDI results are presented here.

For validation against real engine results, the XPNO_x model was run at various AVL modes and its predictions compared with measured data. Figure 7 shows that these agreed well at modes 3, 4, 6, 7, and 8, with errors under 20%. The model was off by about 80% at mode 5. The predicted mode-weighted NO_x based on numerical results from modes 3-8 was within 10% of the engine. The model uses cylinder pressure data from cylinder 1 only. This approach is reasonable as long as all six cylinders have nearly identical pressures. However, in some cases significant cylinder-to-cylinder variations may occur owing to differences in the injection timing and EGR distribution.

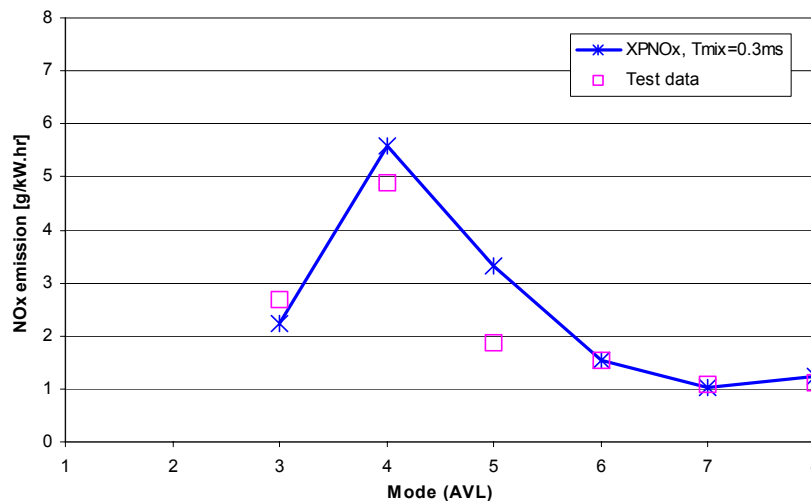


Figure 7: NO_x Emissions Prediction Compared with Measurements for AVL Modes 3-8

XPNO_x did not give meaningful results at modes 1 and 2 because the computer program fails to converge to a solution at low loads, perhaps owing to errors in the inputs. Because the vast majority of cycle NO_x is from modes at which XPNO_x operates well, the tool will be useful for concept-level work. More accurate measurements of EGR flow, cylinder pressure, air/fuel ratio, fueling rate, and fuel injection timing will likely improve the stability of the code at low load. Although not exact, the validated XPNO_x model will be a useful predictor of NO_x emissions.

Investigation of EGR Maldistribution

EGR maldistribution between cylinders could adversely affect engine optimization. It also affects the accuracy of the NO_x prediction model because the model assumes a uniform EGR rate for all cylinders. EGR maldistribution has two causes: 1) poor mixing between the EGR and intake air, and 2) The effects of cylinder firing order and pressure pulsations in the intake and exhaust manifolds. The second effect was quantified using GT-Power at AVL modes 3, 5 and 8 (Figure 8). Even if perfect mixing between air and

EGR is assumed, cylinder phasing and pressure pulsations are likely to contribute about 1%-3% variation in the EGR rate between the cylinders.

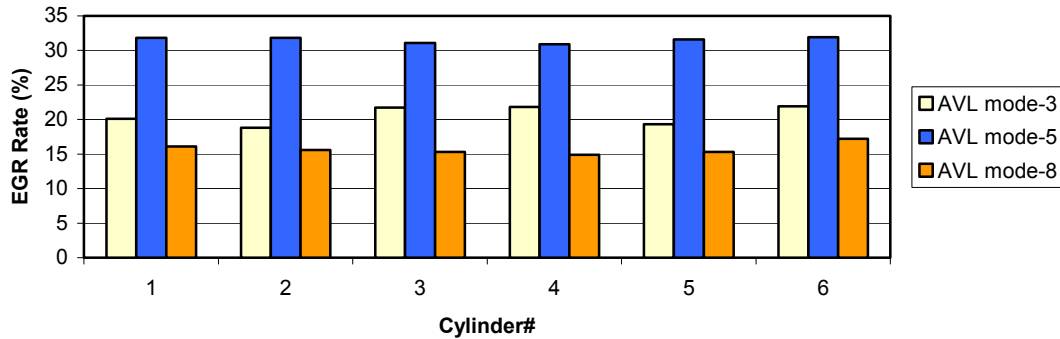


Figure 8: Distribution of EGR Between Cylinders at AVL Modes 3, 5, and 8

Investigation of Shortened Heat Release at High Load

Engine test data at AVL mode 8 show a long tail on the heat release, indicating that the combustion period is too long; this will hurt the engine fuel efficiency. GT-Power was used to assess the effect of faster combustion on engine performance and efficiency. Two cases were run: 1) original rate of heat release from test data, and 2) modified rate of heat release with the combustion tail cut at 60-degrees CA after top dead center (ATDC). The profiles used are shown in Figure 9.

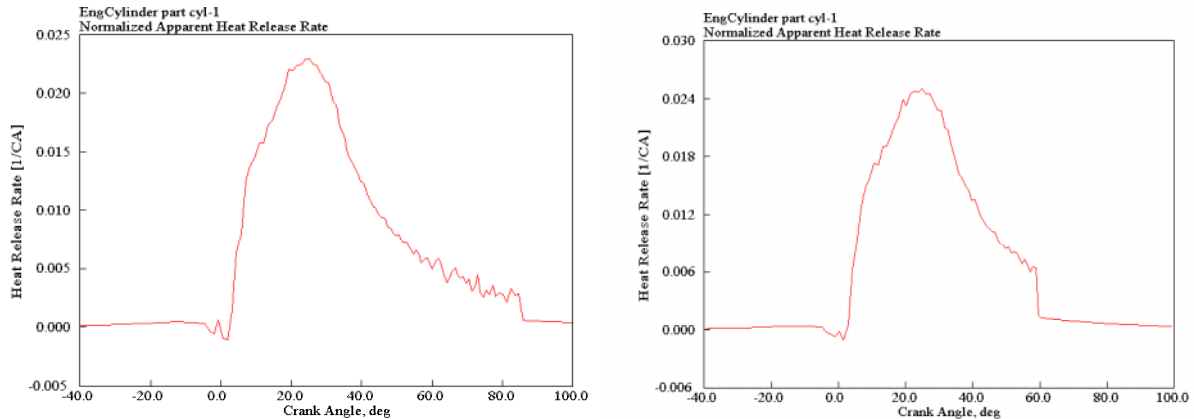


Figure 9: Original and Modified Rate of Heat Release Profile at AVL Mode 8

The shorter heat release period resulted in a 4% increase in engine indicated mean effective pressure (IMEP) and a 5% decrease in indicated specific fuel consumption (ISFC). The EGR rate was almost unchanged. The peak cylinder pressure increased by 2.3%. This suggests that it is beneficial to reduce the “tail” of the heat release.

Investigation of Smaller Compressor Trim

At AVL mode 4 (984 RPM, 84% torque), the engine was found to be operating very close to the compressor surge limit, resulting in instabilities in the air handling controls.

This is aggravated when the EGR rate is increased by closing the VGT turbine ring gap. One option is to try a smaller compressor to move the operating point away from the surge line. The GT-Power model was run at AVL mode 4 with two different compressor maps. As seen in Figure 10, a smaller compressor moved the operating point away from the surge line. The predicted IMEP, ISFC, and EGR are unchanged. A smaller compressor will allow better VGT control and higher EGR rates.

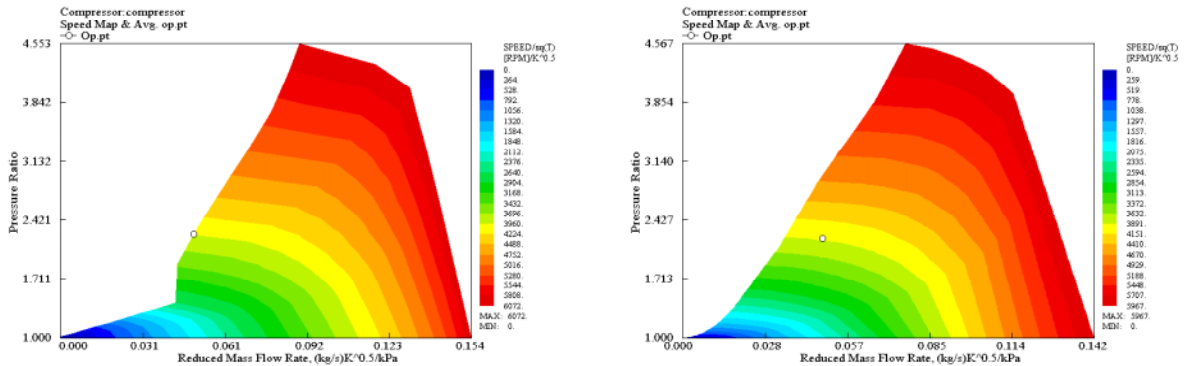


Figure 10: Original and Smaller Compressor Speed Maps with AVL Mode 4 Operating Point

As a next step, the model was run with the smaller compressor at AVL mode 8 to assess its suitability at high load. The result is shown in Figure 11. The engine performance was unchanged, but the operating point moved further away from the surge line. These results suggest the engine would benefit from using a smaller trim compressor.

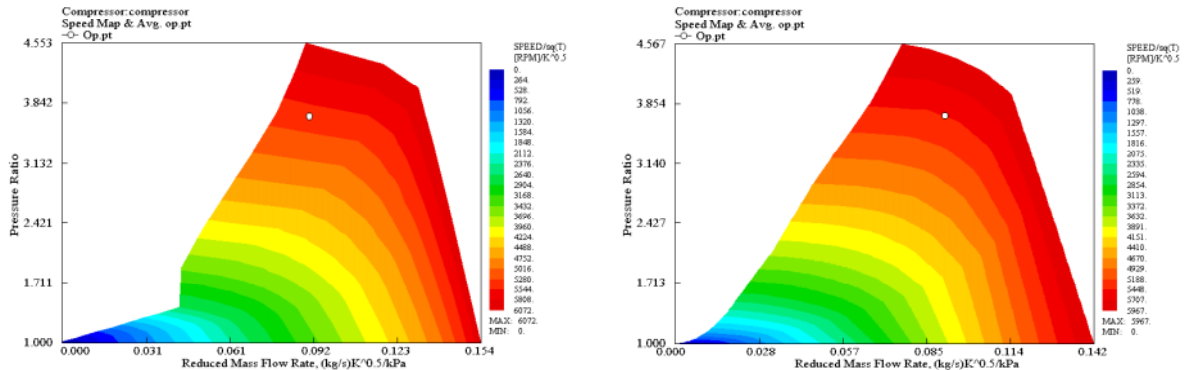


Figure 11: Original and Smaller Compressor Speed Maps with AVL Mode 8 Operating Point

Effect of VGT Turbine Rack Position on EGR Rate

The turbocharger has a variable turbine nozzle ring gap that changes the flow area inlet to the turbine. One method of driving more EGR is to vary this ring gap. By reducing the ring gap, the exhaust pressure is increased, which drives more EGR. However, the compressor also spins faster and drives more fresh air. The GT-Power model was run at different ring gap positions at AVL mode 8 to assess the effects. In Figure 12, the EGR

rate increases to 25% as the turbine ring gap is closed. The IMEP and ISFC are unchanged.

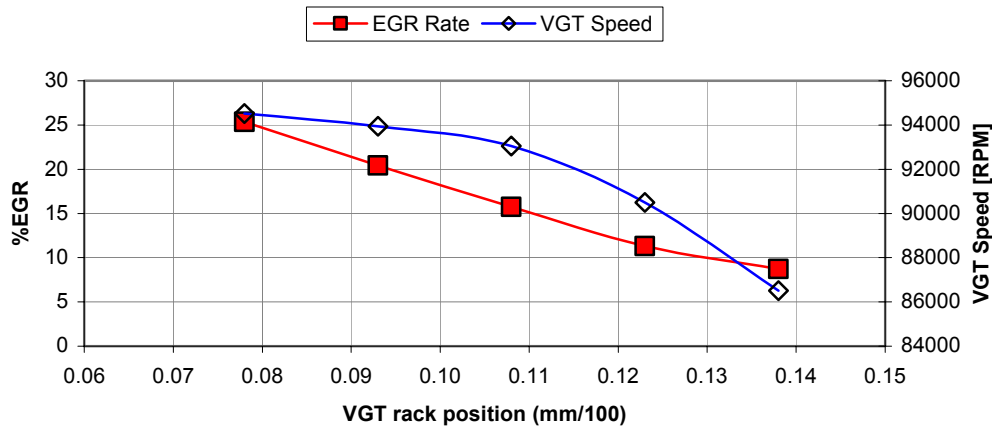


Figure 12: Effect of Turbine Ring Gap (Rack Position) at AVL Mode 8 on EGR Rate and VGT Speed

The effect of closing the ring gap on the compressor operating point is shown in Figure 13. The standard compressor will be surge limited when trying to drive high EGR rates even at the highest engine speeds.

The GT-Power model was also run at AVL mode 4 to see the effect of turbine ring gap on EGR rate and engine performance. In this case, the engine was modeled with the smaller compressor shown in Figure 11 to bring the compressor away from the surge line.

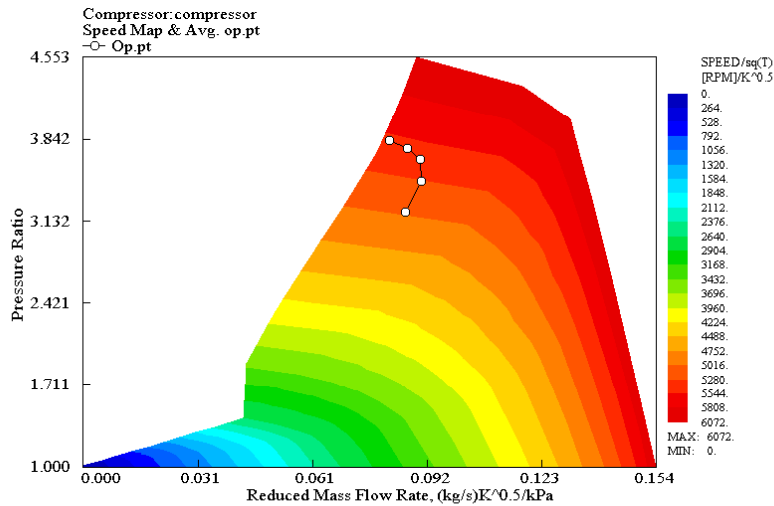


Figure 13: Standard Hardware Compressor Speed Map and Operating Points at Various Turbine Ring Gaps (at AVL Mode 8)

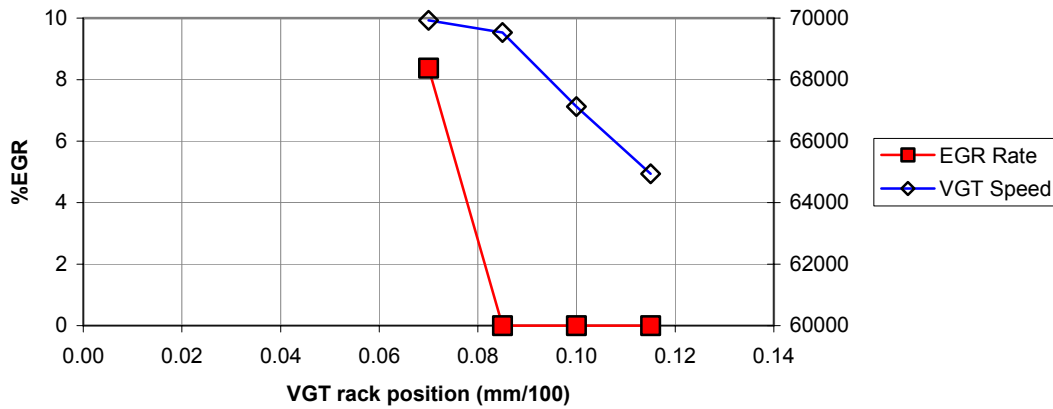


Figure 14: Effect of Turbine Ring Gap (Rack Position) on EGR Rate and Cylinder Peak Pressure with Smaller Compressor Trim (at AVL Mode 4)

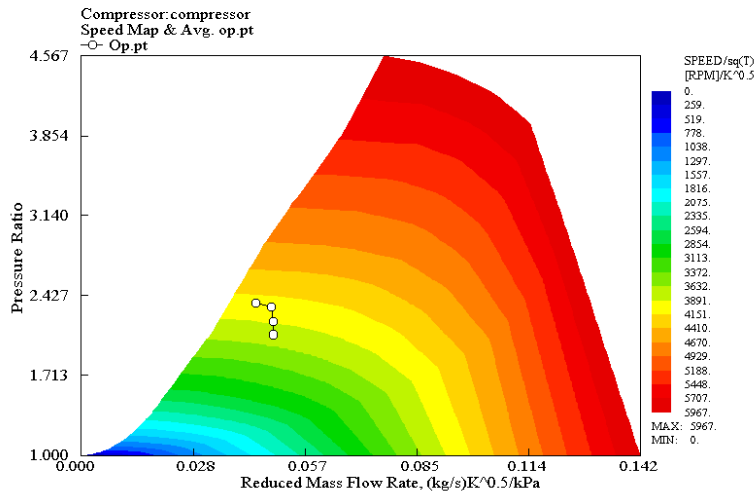


Figure 15: Smaller Trim Compressor Speed Map and Operating Points at Various Turbine Ring Gaps (at AVL Mode 4)

In this case (Figure 14), the EGR rate remained zero until the ring gap was closed below 0.085. It increased to about 8% at a ring gap of 0.07 (i.e., 7 mm gap). The compressor map (Figure 15) shows that the smaller compressor provides sufficient surge margin even when the rack is closed and the mass flow rate through the compressor is reduced. The IMEP and ISFC are unchanged.

Effect of a Larger EGR Valve on EGR Rate

With a fixed VGT setting and the EGR valve fully open at AVL mode 8, the EGR rate is 15%. The current EGR valve is 44 mm in diameter. The GT-Power model was run with a larger EGR valve (50 mm, 30% more flow area) at the same operating conditions. As seen from Figure 16, a 30% increase in EGR valve flow area does not increase the EGR rate appreciably. The existing EGR valve size is sufficient and is not limiting the EGR rate.

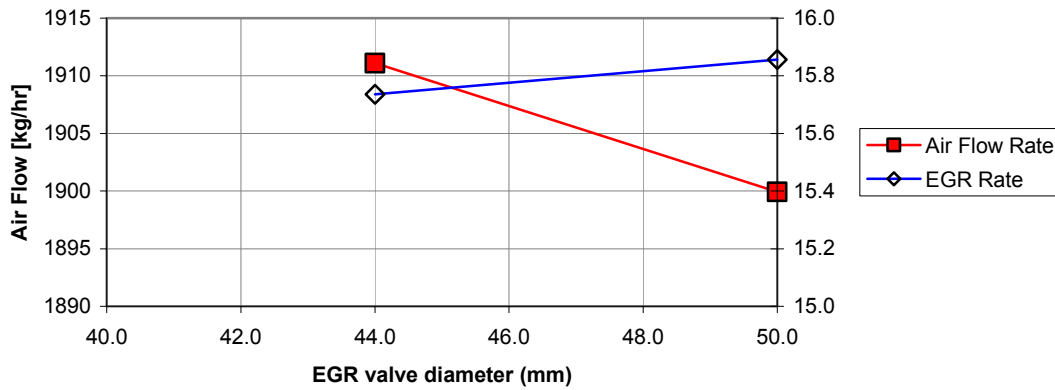


Figure 16: Effect of EGR Valve Diameter on Airflow Rate and EGR Rate at AVL Mode 8

Effect of a Smaller Turbine

The ISX engine has several ratings from 400-565 bhp. The standard VGT turbine is sized to allow operation up to the highest rating, but it may not be the best choice at lower power (450 bhp) and higher EGR rates. The engine model was run at AVL mode 8 with different turbines by scaling the turbine map with factors of 0.8, 1.0 (baseline), and 1.2. A factor of 0.8 applied to the turbine mass flow rate simulates a smaller turbine, which increases the EGR rate from 16% to 27%. IMEP and ISFC are unchanged. Comparing Figure 17 and Figure 18 with earlier results (Figure 12 and Figure 13) shows that the effect is similar to closing the turbine ring gap.

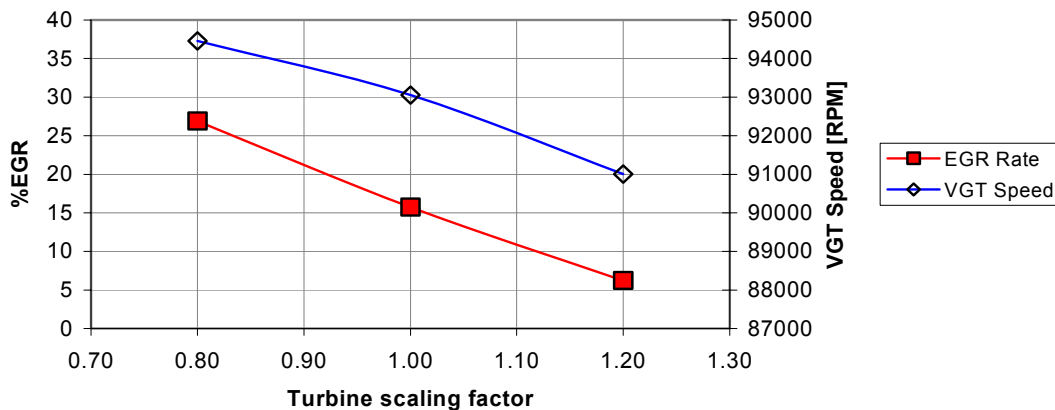


Figure 17: Effect of VGT Turbine Size on EGR Rate and VGT Speed at AVL Mode 8

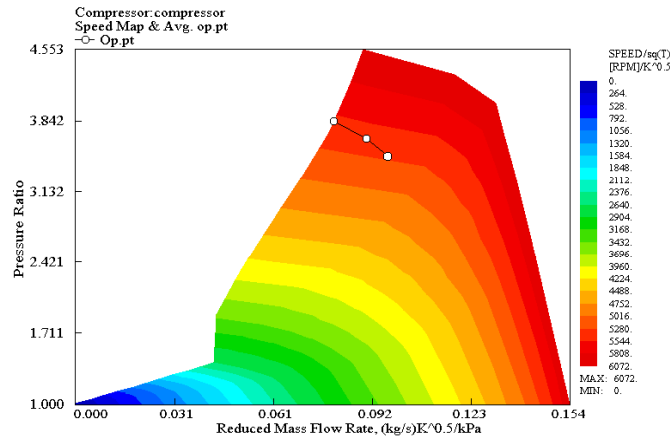


Figure 18: Effect of VGT Turbine Size on the Compressor Operating Point at AVL Mode 8

EGR Introduction: Comparison Between a Venturi and Reed Valve

Presently, the ISX uses a venturi in the inlet system to draw in EGR from the exhaust. However, pressure pulsations in the exhaust can be used to introduce EGR into the inlet system via a reed valve. In a six-cylinder, four-stroke engine there are six pressure pulses in the exhaust system per engine cycle and two revolutions per cycle. A reed valve leading to the inlet manifold would open briefly during each exhaust pressure pulse, sending EGR into the inlet. To study this alternative, the engine was modeled with a reed valve at AVL mode 8, and the results were compared with a standard model with the venturi. The EGR valve was kept fully open in both cases. The venturi and the reed valve provided very similar EGR rates (~ 19%) and identical IMEP and ISFC. There is no performance benefit from using a reed valve instead of the current hardware for introducing EGR.

EGR Introduction: Combination Venturi and Reed Valve

The model was modified to have a venturi and a reed valve. This was run at AVL modes 4 and 8 and the results compared with the standard system with a venturi only. The addition of a reed valve increased the EGR rate by 5% (AVL mode 4) and 2.4% (AVL mode 8). IMEP and ISFC were unchanged. This suggests only a marginal benefit in EGR rate with the addition of a reed valve.

Effect of Modified EGR Venturi

The diffuser angle of the standard EGR venturi is 12 degrees. The GT-Power model was run at AVL mode 8 with a diffuser angle of 6 degrees. A gentler diffuser angle should improve pressure recovery downstream of the venturi and thereby improve engine performance by reducing inlet system pressure losses. However, the model predicted no change in engine IMEP and ISFC. EGR rate increased slightly from 16% to about 17%. In reality, a wide diffuser angle (12 degrees) is likely to suffer from flow separation at the wall and result in loss of pressure recovery. The GT-Power model is not designed to

handle this and so cannot predict a change in performance in this case. Computational fluid dynamics simulation or actual engine tests are required for further understanding.

The throat of the EGR venturi accelerates the gas flow, resulting in the low-pressure region necessary to draw EGR into the intake line. The GT-Power model was run at AVL mode 8 with its original venturi throat diameter and a diameter with nearly 55% less flow area. As hoped, with the smaller diameter the EGR rate increased, in this case from 16% to 23% (Figure 19).

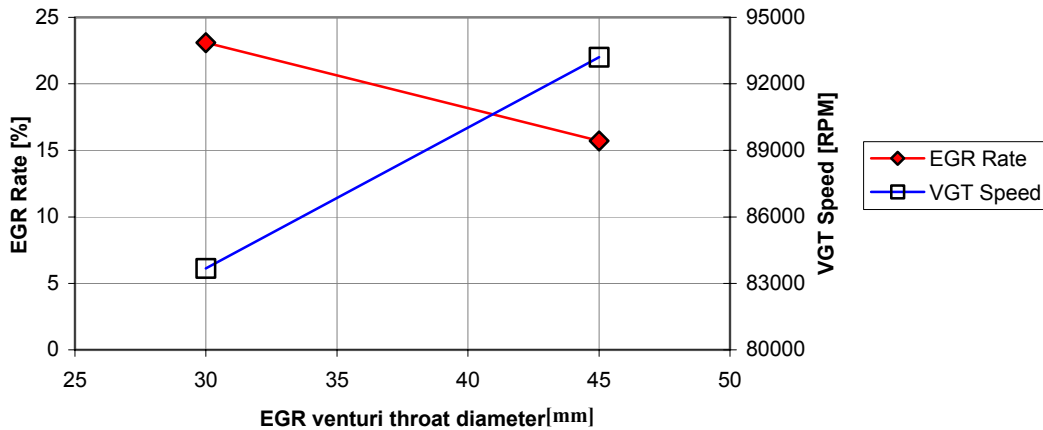


Figure 19: Effect of EGR Venturi Throat Diameter on EGR Rate and VGT Speed at AVL Mode 8

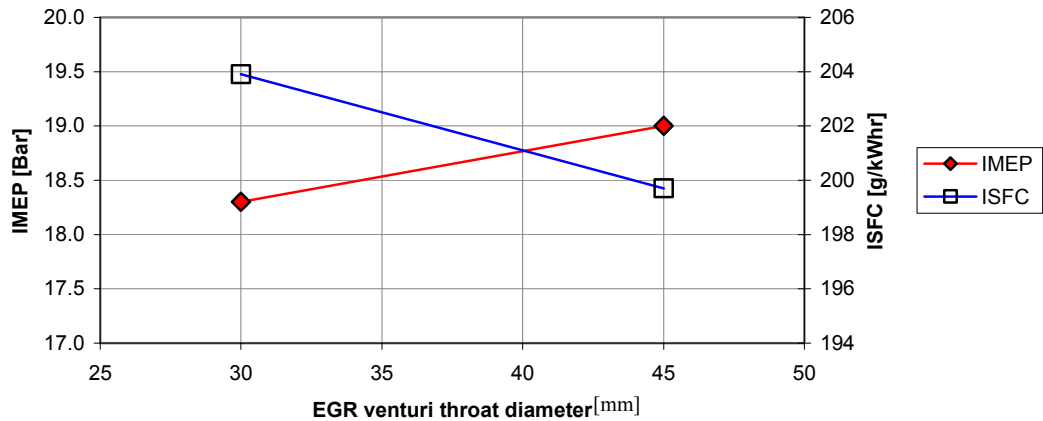


Figure 20: Effect of EGR Venturi Throat Diameter on IMEP and ISFC at AVL Mode 8

However, the smaller throat reduced the IMEP by 3% and increased the ISFC by 2% (Figure 20). Reducing the throat diameter will increase the EGR rate but with a performance penalty.

GT-Power: Summary of Potential Engine Modifications

The advantages and disadvantages of the modeled hardware changes are summarized in Table 1.

Table 1: Summary of Potential Engine Modifications

Potential Modification	Advantages	Disadvantages	Potential Option for Future?
Improve EGR distribution between cylinders	Optimizes NO _x reduction and improves engine performance	Performance—none, could impact engine package	Yes
Shorter heat release period at high-speed/high-load points	Improves fuel economy	None	Yes
Switch to a smaller compressor in VGT	Better surge margin	Ambient conditions—none, may impact off-ambient robustness	Yes
Close the VGT turbine rack or use smaller turbine	Helps drive high levels of EGR	Could lead to VGT over-speed at high-speed/high-load operation	Yes
Use a larger EGR valve	None detected	Less resolution at low lift	No
Use a reed valve to drive more EGR	Mechanically simple device	Not likely to provide high EGR levels at high-speed/high-load points	No
Use a reed valve in combination with a venturi to drive more EGR	No significant increase in EGR rate over a venturi	Increased complexity	No
Modify EGR venturi diffuser	Improves pressure recovery in the intake line	Limited space to install a longer diffuser	Yes
Modify EGR venturi throat	Improves suction leading to significantly more EGR	Fuel efficiency penalty	Yes

Method of Achieving Ultra-Low NO_x Emissions

Screening of various concepts to meet the 0.5g/bhp-hr NO_x target was carried out with the GT-Power and XPNOx models, and hardware changes were identified. A smaller turbocharger compressor will improve the compressor surge margin as the EGR rate is increased. Simulations were run at the AVL 8-mode points, producing target engine settings to achieve the 0.5g/bhp-hr NO_x target over the AVL 8-mode test. The effect on fuel efficiency was also estimated.

Figure 21 shows the effect if injection timing retard is required in addition to high EGR. The high EGR strategy reduces the NO_x to 0.5 g/bhp-hr with about a 2% efficiency penalty. An additional 5-degree retard reduces the NO_x to about 0.3 g/bhp-hr, but the efficiency penalty increases to 7%. Given validation experience, it is expected that the NO_x predictions are accurate within 10%-20%. A fuel consumption penalty of 4% is probably a realistic target at this stage.

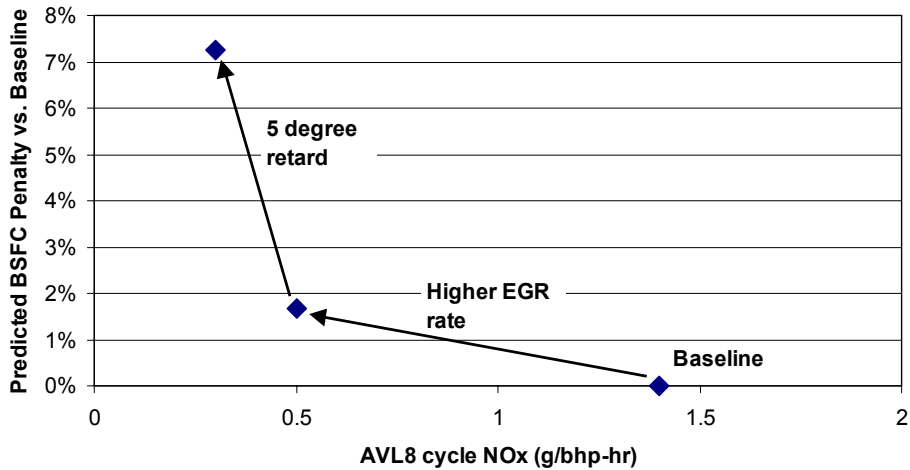


Figure 21: Impact of Injection Timing Retard on Fuel Efficiency Penalty

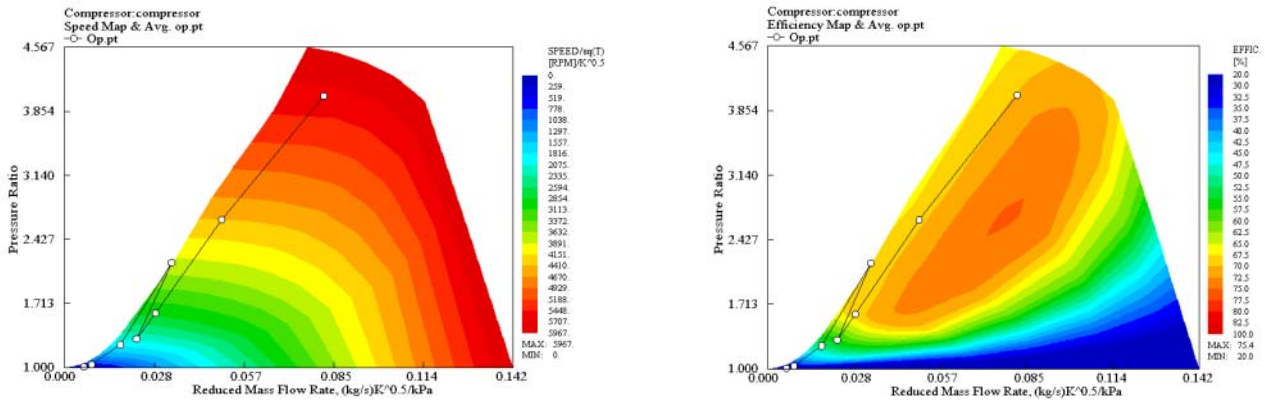


Figure 22: 0.5 g/bhp-hr NO_x Model of AVL Test Points on Smaller Trim Compressor Speed and Efficiency Maps

Figure 22 shows the AVL 8-mode operating points on the VGT compressor speed and efficiency maps. To avoid surge, the original compressor map was replaced with that of a smaller compressor. Even with this change, the 0.5-g NO_x recipe with higher EGR rates and reduced airflow rates pushes the operating points close to the surge line.

3.3 Diesel Baseline Testing

3.3.1 Objective

Baseline testing was conducted to establish the emissions and performance of the diesel engine with EGR and to check data repeatability. Tests were performed at operating points representative of the full engine map, with emphasis on those points that are most critical to NO_x production.

3.3.2 Accomplishment Summary

The engine was tested with diesel fueling and EGR over two standard test cycles using the standard calibration. The AVL 8-mode cycle-weighted NO_x emissions were 1.97 g/bhp-hr. The ESC 13-mode emissions were 2.28 g/bhp-hr. This was an early development calibration, and the results are not necessarily indicative of current production diesel ISX engines with EGR.

3.3.3 Accomplishment Details

AVL 8-Mode Test Cycle

The AVL 8-mode test is a steady-state test designed to correlate closely with the emission results from the Federal Test Procedure (FTP) heavy-duty transient test (Figure 6). The cycle-weighted NO_x emissions were 1.97 g/bhp-hr using the calibration provided. This was an early development calibration, and the results are not necessarily indicative of current production diesel ISX engines with EGR. Table 2 shows a mode-by-mode breakdown.

There were very low EGR rates at mode 4; this likely accounts for the high NO_x emissions at this mode. Early in the testing program, operating instabilities were encountered with the VGT and air handling system near this operating point. Hardware changes made later in the program removed any instabilities.

Table 2: AVL 8-Mode Test Results under Diesel Fueling

AVL Mode	Speed (rpm)	Load (%)	BSNO_x (g/bhp-h)	BSnmHC (g/bhp-h)	BSCO (g/bhp-h)	BSCH₄ (g/bhp-h)	Diesel BSFC (g/bhp-h)
2	732	25	3.31	0.25	0.74	0.00	190.6
3	854	63	3.28	0.10	0.24	0.00	165.9
4	984	84	5.81	0.07	0.12	0.00	165.9
5	1800	18	2.95	0.44	1.12	0.00	256.4
6	1740	40	1.30	0.24	0.79	0.00	191.9
7	1740	69	1.26	0.13	0.58	0.00	185.5
8	1668	95	1.30	0.07	0.34	0.00	180.5
Composite Results			1.97	0.18	0.64	0.00	194.9

ESC 13-Mode Test Cycle

The ESC is a steady-state test with 13 modes (Figure 23). It is used in the Supplemental Emissions Test as part of the EPA certification procedures for heavy-duty on-highway engines. The test points are uniformly distributed under the torque curve, making it a useful test for mapping the engine calibration.

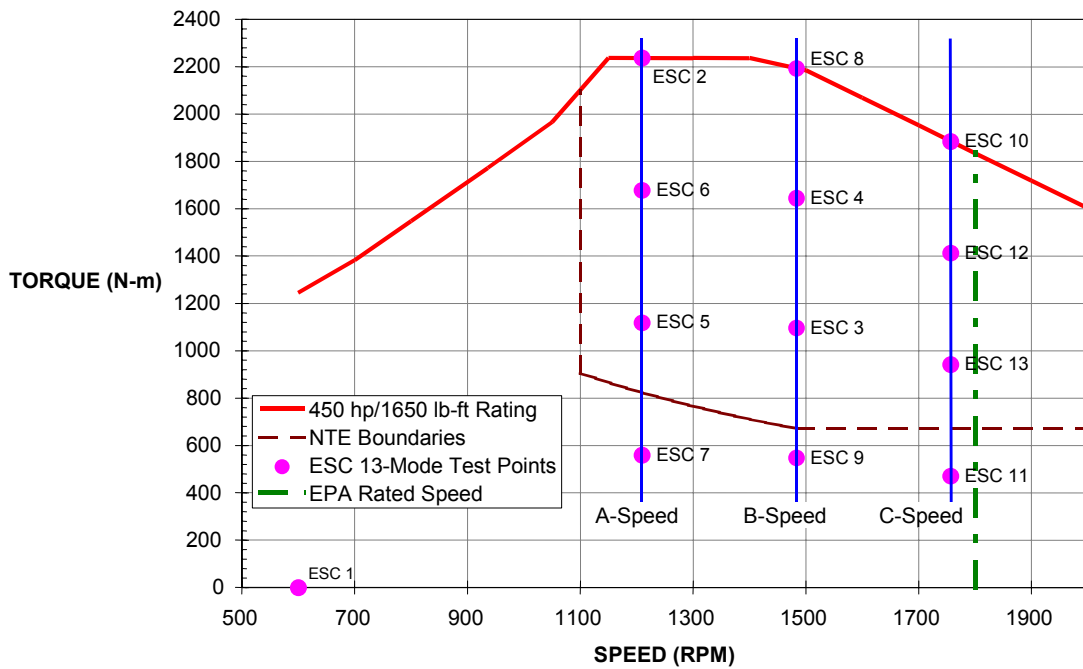


Figure 23: ESC 13-Mode Test Points and Torque Curve

The ESC cycle-weighted NO_x emissions were 2.28 g/bhp-hr with diesel fueling using the calibration provided. Like the AVL results, this was an early development calibration, so the results are not necessarily indicative of current production diesel ISX engines with EGR. Table 3 shows a mode-by-mode breakdown.

Table 3: ESC 13-Mode Test Results under Diesel Fueling

ESC Mode	Speed	Load (%)	BSNO _x (g/bhp-h)	BSnmHC (g/bhp-h)	BSCO (g/bhp-h)	BSCH ₄ (g/bhp-h)	Diesel BSFC (g/bhp-h)
2*	A	100	1.40	0.06	1.24	0.00	160.2
3	B	50	2.22	0.09	0.42	0.00	165.4
4	B	75	2.23	0.06	0.43	0.00	155.2
5	A	50	3.34	0.08	0.69	0.00	156.1
6	A	75	2.01	0.05	0.58	0.00	155.1
7	A	25	3.81	0.16	0.42	0.00	168.5
8	B	100	1.76	0.04	0.47	0.00	159.2
9	B	25	2.85	0.14	0.49	0.00	184.2
10	C	100	1.88	0.05	1.03	0.00	157.1
11	C	25	4.02	0.19	0.41	0.00	214.2
12	C	75	1.93	0.06	0.86	0.00	159.6
13	C	50	3.37	0.11	0.29	0.00	173.2
Composite Results			2.28	0.07	0.69	0.00	162.8
* Note: At mode 2 maximum torque reached 88% instead of 100%							

3.4 HPDI Baseline Testing

3.4.1 Objective

The diesel fuel system hardware was replaced with the HPDI fuel system for natural gas fueling. Baseline testing was conducted to determine the initial performance and emissions of the HPDI engine with EGR and to confirm functionality of the HPDI fuel system with EGR.

3.4.2 Accomplishment Summary

The HPDI fuel system was installed on the engine, and an initial calibration was developed using basic timing and EGR rate swings. The engine was tested over the AVL 8-mode test with the original J-31 injectors and a constant fuel pressure of 23 MPa. The cycle-weighted results were 1.46 g/bhp-hr for NO_x with a 177.6 g/bhp-hr diesel-equivalent fuel consumption. These tests were conducted early in the development program and are not necessarily optimal.

The J-31 injectors were replaced with newer J-34 injectors, and three injector tips with different nozzle geometries were tested. An injector tip using an 18-degree, 0.72-mm diameter nozzle geometry was selected as the most suitable of the three.

3.4.3 Accomplishment Details

HPDI Hardware Conversion

The production diesel fuel system was removed from the engine and replaced with a pre-production HPDI fuel system, including the following:

- An integrated fuel supply module (IFSM) that regulates high-pressure diesel and natural gas and delivers them to the fueling rails in the head
- A fuel pump for delivering high-pressure diesel to the IFSM
- J-31 HPDI fuel injectors, which are solenoid actuated
- An intelligent driver module (IDM), which includes the electronic controls for the HPDI system
- The necessary wiring harnesses

The IFSM (Figure 24) is situated on the air inlet side of the head. The high-pressure diesel is manually regulated from 15-25 MPa. The natural gas pressure is regulated by the dome-loaded self-relieving regulator to a pressure slightly lower than the diesel pressure, to ensure that no natural gas leaks into the diesel side of the injector. Diesel is supplied to the IFSM by a high-pressure fuel pump driven from the engine crankshaft (Figure 25).



Figure 24: Photograph of the IFSM Assembly



Figure 25: High-Pressure Diesel Fuel Pump

The stock diesel fuel injectors, which are actuated by a cam and rockers, were removed along with the valve rocker assembly, and the J-31 HPDI fuel injectors (Figure 26) were installed (Figure 27).



Figure 26: The J-31 HPDI Injector

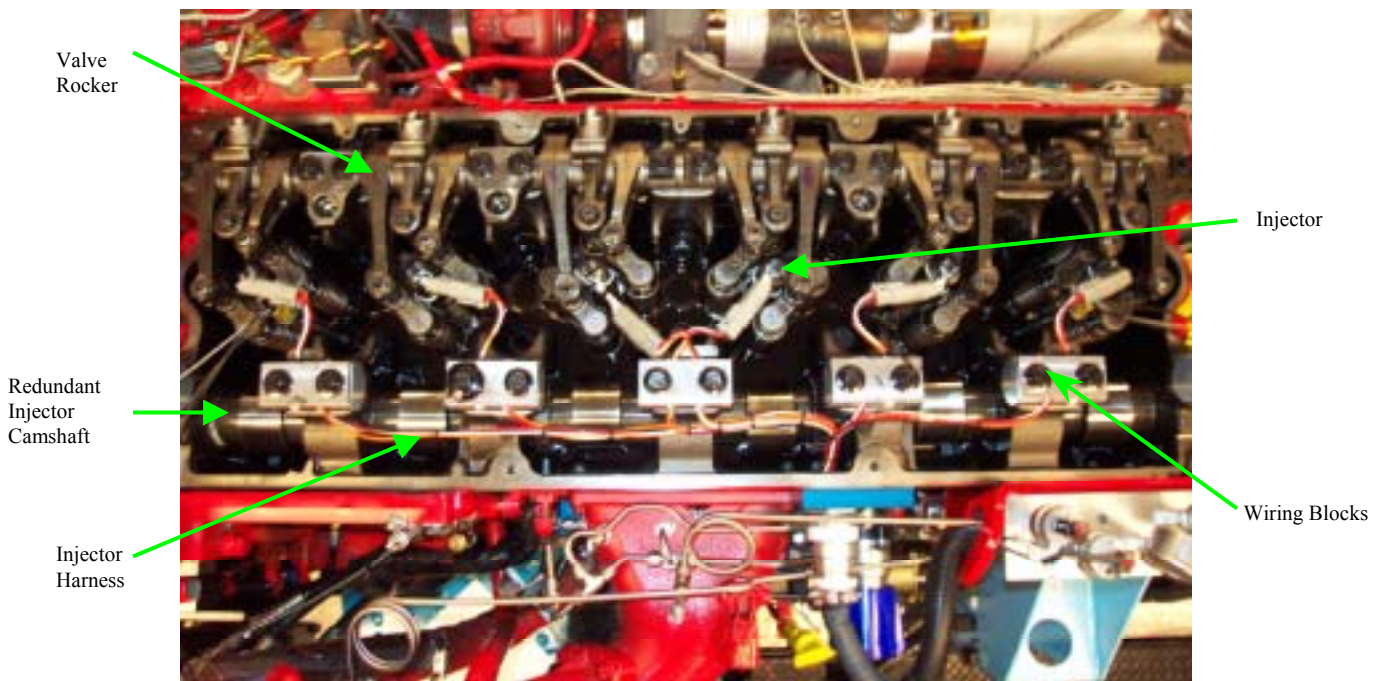


Figure 27: Installed J-31 Injectors and Wiring Harness

The control architecture is incremental, meaning the existing Cummins CM870 ECM drives an added Westport IDM, which further modifies some of the output signals. Figure 28 shows the signals that the injector receives from the Westport IDM controller.

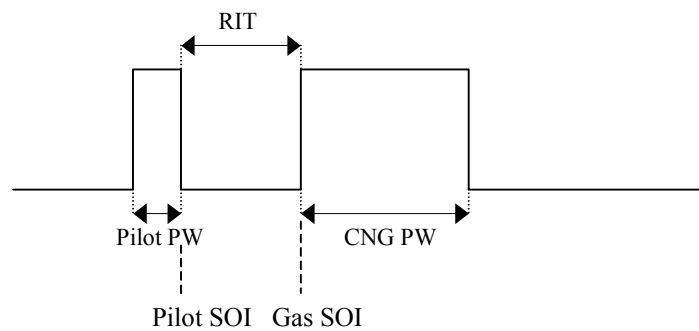


Figure 28: Injection Pulse and Timing Diagram

Inherent in any “common rail” type injector with electro-hydraulic actuation is a delay between commanded timing and actual fuel delivery. The timing offset can be used to compensate for injection delay or differences in injection rate shape between the baseline diesel and gas engines.

Preliminary HPDI Calibration: AVL 8-Mode Test Cycle

After installation of the HPDI fuel system, the engine was recalibrated for initial operation. Basic timing and EGR swings were conducted at all AVL and some ESC modes to give good coverage of the engine speed and load range. New timing and EGR fraction maps were determined from the tradeoff between fuel consumption and NO_x emissions, with the carbon monoxide (CO) emissions also monitored to ensure that they were not excessive. Fuel pressure was maintained at 23 MPa. The resulting HPDI calibration had slightly higher EGR rates than the diesel calibration. The resulting AVL 8-mode weighted NO_x emissions were 1.46 g/bhp-hr. A breakdown of the AVL 8-mode test results is given in Table 4.

Table 4: AVL 8-Mode Test Results under HPDI Fueling with Initial Calibration

AVL Mode	Speed (rpm)	Load (%)	Measured EGR Fraction (%)	BSNO _x (g/bhp-h)	BSnmHC (g/bhp-h)	BSCO (g/bhp-h)	BSCH ₄ (g/bhp-h)	Diesel Equivalent BSFC (g/bhp-h)
2	732	25	27.2	4.16	0.20	1.98	1.80	172.6
3	854	63	22.3	2.14	0.09	1.20	0.61	151.0
4	984	84	8.1	3.22	0.05	0.91	0.22	145.3
5	1800	18	30.1	2.55	0.29	2.99	4.29	248.2
6	1740	40	30.0	0.99	0.16	2.03	2.58	180.2
7	1740	69	23.6	0.77	0.07	1.11	1.28	169.2
8	1668	95	15.0	0.80	0.06	1.21	0.55	173.0
Composite Results			--	1.46	0.11	1.52	1.46	177.6

This initial testing showed that at low speed and load conditions, NO_x emissions are reduced as the gas rail pressure (GRP) is reduced, so fuel pressure becomes a variable in later tests.

Injector Upgrade

After initial testing with J-31 injectors, newer J-34 HPDI fuel injectors became available, so the engine was upgraded to these. Improvements in the J-34 include the following:

- Improved design for manufacture
- Increased injection pressure capability
- Better pilot injection flexibility

The increased injection pressure capability allows a faster injection rate, especially at high speed and high load, where the heat release period is critical in diesel-cycle engines. The tables in the Westport controller were modified to suit the characteristics of the J-34 injectors.

Nozzle Geometry Selection

The match between the injector nozzle geometry and the combustion system (combustion bowl, in-cylinder air motion, and ignition source) is critical in any late-cycle, direct injection engine (HPDI, diesel, and gasoline direct injection). Therefore, three different HPDI nozzle configurations were tested and evaluated.

Results from earlier non-EGR ISX test programs showed that a 15-degree nozzle matches this combustion system, so two sets of nozzles were configured with a 15-degree angle. Each set had a different jet hole diameter (0.72 mm and 0.77 mm were tested), giving a difference in injection rate and jet penetration, the typical distance traveled by the fuel jet into the cylinder. Injectors of 18 degrees were also tested with holes of 0.72 mm—these gave the best overall results, so all future work used this configuration.

3.5 Preliminary Optimization: EGR Rate, Injection Timing, Fuel Pressure

3.5.1 Objective

Initial performance and emissions optimization was conducted by varying the EGR rate, injection timing, and fuel pressure. The relationship between these parameters and engine performance and emissions was examined to determine areas where further optimization and refinements are most needed.

3.5.2 Accomplishment Summary

EGR rates were varied from approximately 8%-30% at constant fuel pressure and injection timing. As expected, NO_x emissions decreased as EGR rates increased but with CO and BSFC penalties. At high loads, NO_x was not reduced as much as desired for the program goals.

Pilot timing and quantity was varied at ESC mode 3 using a constant fuel pressure of 23 MPa. In general, as the pilot quantity decreased and the relative injection timing (RIT) increased, the combustion of the main gas charge became more erratic. This poor gas combustion adversely affects emissions and fuel consumption. Pilot injection quantities of 5-10 mg per injection provide the best tradeoff of emissions and efficiency without adversely affecting combustion.

GRP was varied from 23-28 MPa at high loads and speeds. The presence of EGR slows the rate of combustion. The increased fuel injection rate resulting from higher fuel pressures increases the rate of combustion. Therefore, as EGR rates increase at higher speeds and loads, the fuel pressure may be increased to control the rate of combustion.

3.5.3 Accomplishment Details

EGR Swings

A five-point EGR swing was conducted with constant fuel pressure and injection timing while the gas pulse width controlled the engine torque. The EGR rate was swung up to +/- 25% of the nominal EGR rate from the diesel-fueled ECM map. As expected, NO_x emissions decreased as EGR rate increased, with some BSFC and CO penalties. The CO

level is an important indicator of combustion quality and onset of incomplete combustion, with considerable CO increases taken as an indication of incomplete combustion. Figure 29 shows these responses at ESC modes 5 and 10.

At mode 5, one of the more difficult not-to-exceed (NTE) conditions at which to achieve low NO_x, the NO_x versus BSFC tradeoff experienced a 5.4% increase in BSFC for a 75% reduction in brake specific NO_x (BSNO_x) by application of up to 30% EGR. The minimum NO_x level achieved was 0.5 g/bhp-hr, well below the 0.75g/bhp-hr limit required to meet NTE requirements for a 0.5g/bhp-hr engine (based on an NTE factor of 1.5, required for engines with NO_x Family Emission Limits below 1.5g/bhp-hr).

Figure 29 also shows the EGR swing data at ESC mode 10. Here the EGR valve is generally fully open, and the only way to increase the EGR rate is to increase the pressure differential across the EGR system by closing the VGT, increasing the backpressure in the exhaust manifold in relation to the boost pressure in the inlet manifold.

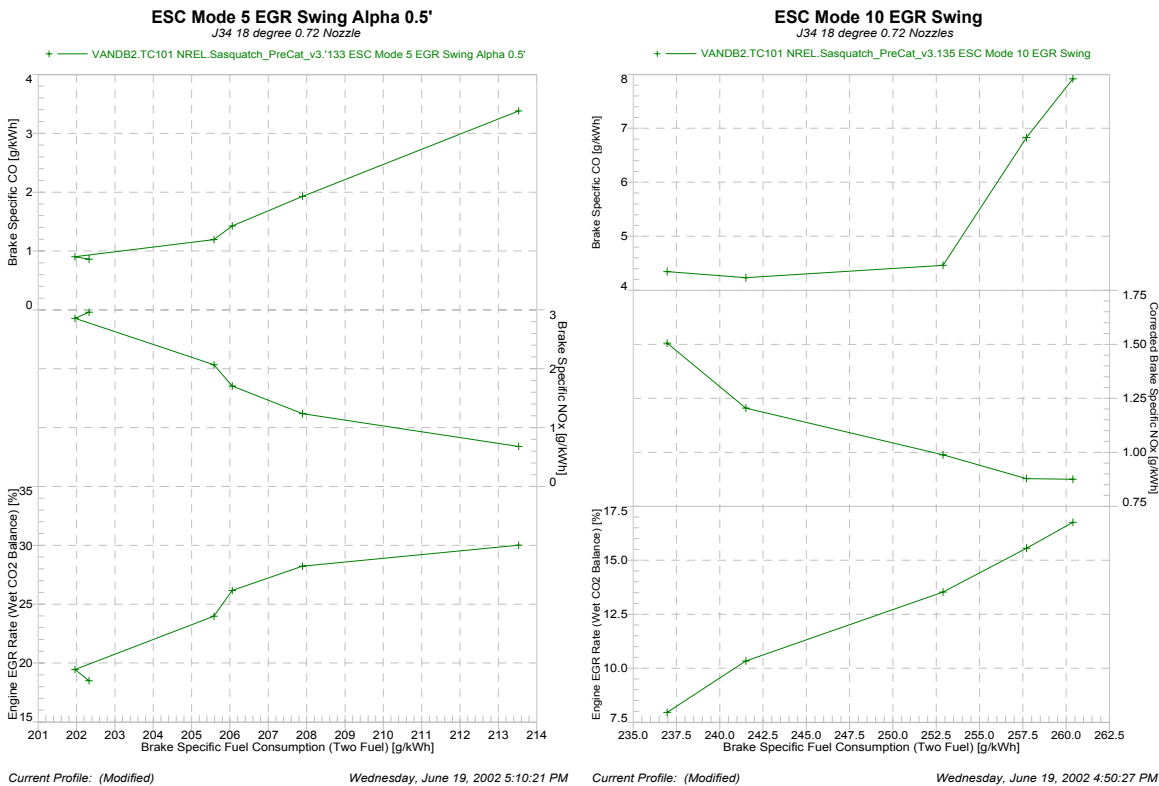


Figure 29: ESC Mode 5 and 10 EGR Swings

The NO_x versus BSFC tradeoff shows that for a 9% increase in BSFC the BSNO_x was reduced by 40% to a minimum level of 0.65g/bhp-hr, close to the target of 0.5g/bhp-hr. The efficiency here was disappointing, and a significant improvement was required to meet the program goals.

Pilot Fueling Swings

Pilot timing and quantity were varied with the objective of minimizing pilot fuel consumption while maintaining good combustion and emissions. Pilot pulse width (PPW) and RIT, the delay between the pilot and gas injection, were varied at ESC mode 3 using

a constant fuel pressure of 23 MPa. This test mode (1,498 rpm and 50% load) is close to on-highway cruise conditions and an important contributor to methane (CH₄) emissions on an ESC test.

EGR rate was kept constant at 30% +/- 1%, and the start of gas injection was kept constant. The gas pulse width was adjusted to maintain a constant torque. The start of combustion was allowed to vary as the PPW and RIT changed. Typically, start of combustion was between top dead center and 5 degrees ATDC.

The tests indicated that pilot injection quantities of 5-10 mg per injection provided the best tradeoff of emissions and efficiency without adversely affecting combustion. Similar tests may be conducted in the future at other operating points.

In general, as the pilot quantity decreases and the RIT increases, the combustion of the main gas charge becomes more erratic. This poor gas combustion adversely affects emissions and fuel consumption. A summary of the results is shown in Table 5, and the performance responses are shown graphically in Figure 30 through Figure 34.

For this application and emissions level, a pilot quantity of 5-10 mg per injection is preferred because of the low BSNO_x, BSFC, and pilot energy ratio. This information will assist in range setting during the later multivariable optimization phase.

Table 5: Summary of Pilot Fueling Swings

Pilot Quantity Range	Positive Impact	Negative Impact	Select/Deselect
0-5 mg/inj	<ul style="list-style-type: none"> Pilot energy ratio < 5% 	<ul style="list-style-type: none"> COV of IMEP up to 5% High CH₄ Large sensitivity to pilot timing 	Deselect —combustion is marginal and close to misfire
5-10 mg/inj	<ul style="list-style-type: none"> Best NO_x vs. BSFC trade off COV of IMEP < 2% Low NO_x Low BSFC Pilot energy ratio < 8% 	<ul style="list-style-type: none"> Higher pilot energy ratio CH₄ variability 	Select for low-NO _x applications where CH ₄ regulations allow
10-15 mg/inj	<ul style="list-style-type: none"> Best BSFC Low CH₄ Low CH₄ sensitivity to timing Low CO potential Good NO_x vs. BSFC 	<ul style="list-style-type: none"> Pilot energy ratio up to 11% 	Select when CH ₄ and CO are critical and NO _x levels can be higher
15-20 mg/inj	<ul style="list-style-type: none"> Lowest COV of IMEP Low CO potential Lowest CH₄ Low CH₄ sensitivity to timing Good BSFC 	<ul style="list-style-type: none"> Poor NO_x vs. BSFC High CO sensitivity Pilot energy ratio up to 15% 	Deselect —pilot energy ratio and NO _x are high

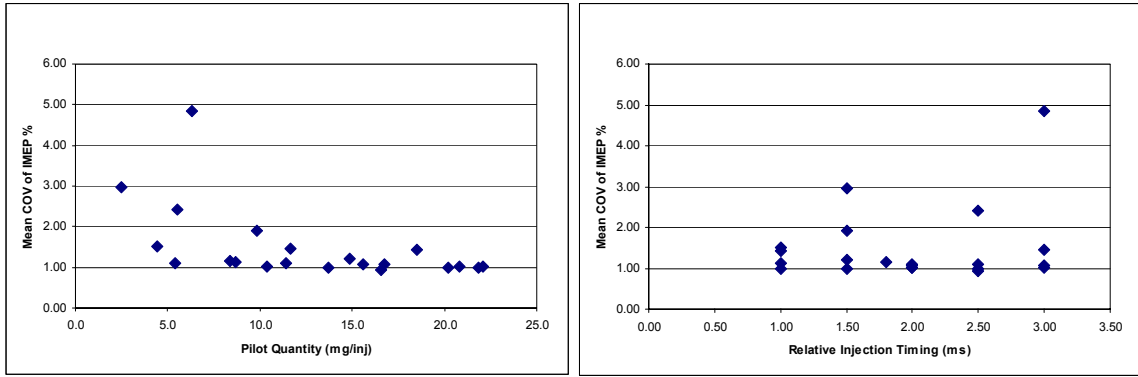


Figure 30: Pilot Fueling Swings—Coefficient of Variance (COV) of IMEP Response

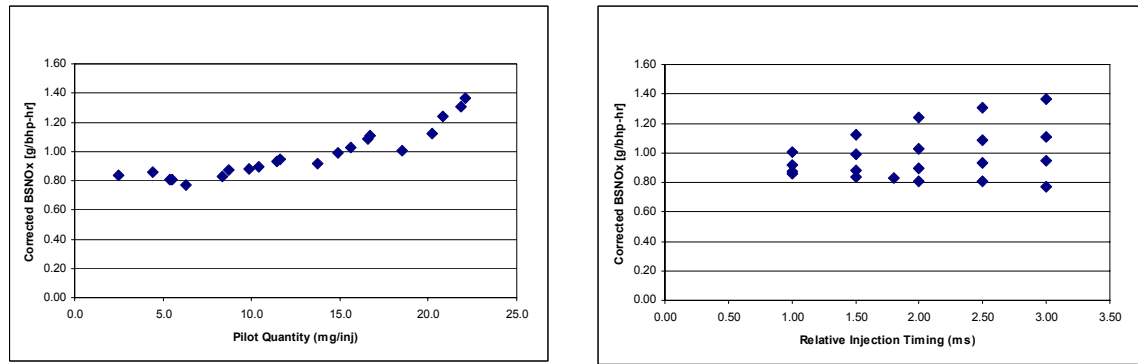


Figure 31: Pilot Fueling Swings—Corrected BSNO_x Response

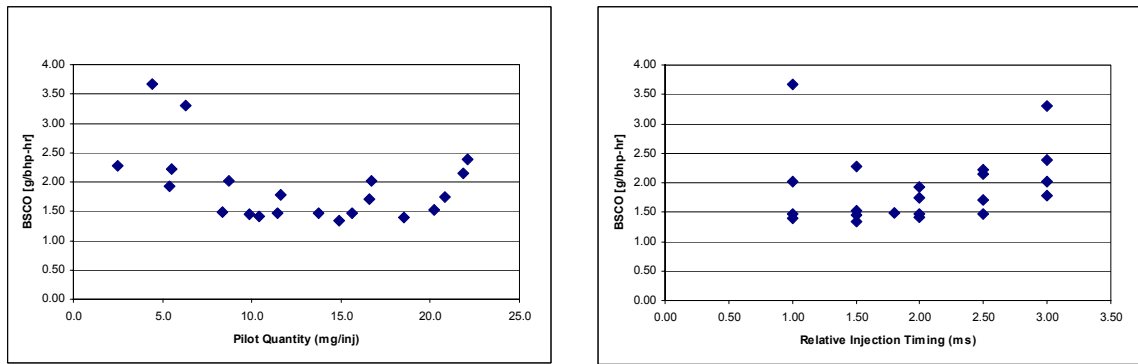


Figure 32: Pilot Fueling Swings—Brake Specific Carbon Monoxide (BSCO) Response

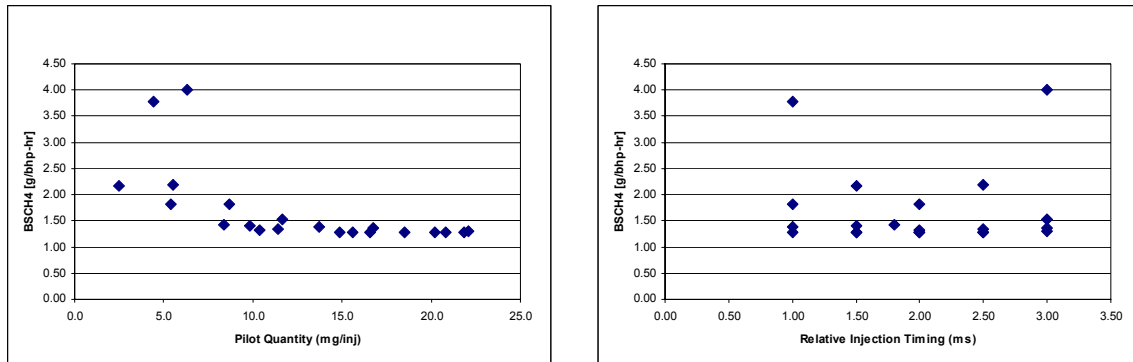


Figure 33: Pilot Fueling Swings—Brake Specific CH₄ (BSCH₄) Response

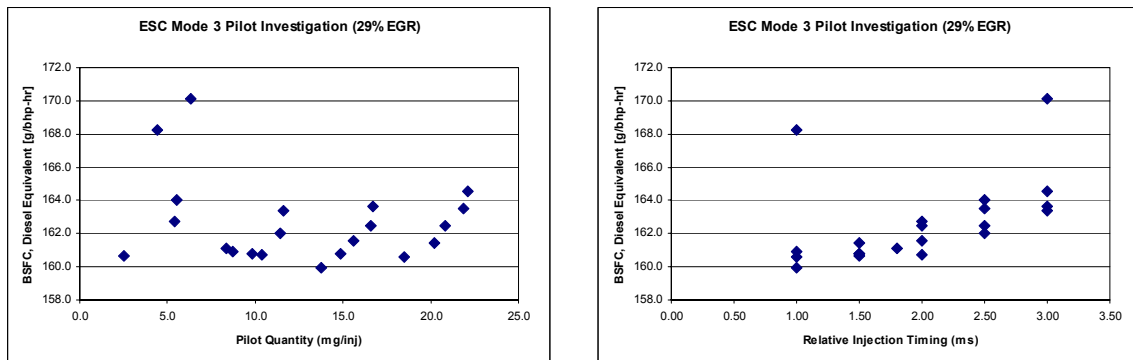


Figure 34: Pilot Fueling Swings—BSFC Response

GRP Swings

High EGR rates are necessary for low NO_x emissions at high loads, but the heat release period increases, resulting in poorer efficiency. Increasing the gas injection pressure, which increases the injection rate, shortens the heat release again.

Tests were conducted at GRPs of 23, 25, and 28 MPa at AVL mode 8 (100% load at 1,668 rpm) and ESC mode 10 (100% load at 1,757 rpm). The EGR rate was held constant at 21% and 16% for the AVL mode 8 and ESC mode 10 tests, respectively.

The results at AVL mode 8 are shown in Figure 35 through Figure 38. Operation at 23 MPa was limited because retarding the timing resulted in the exhaust gas temperature (EGT) exceeding its limit, whereas advancing the timing resulted in exceeding the maximum allowable cylinder pressure.

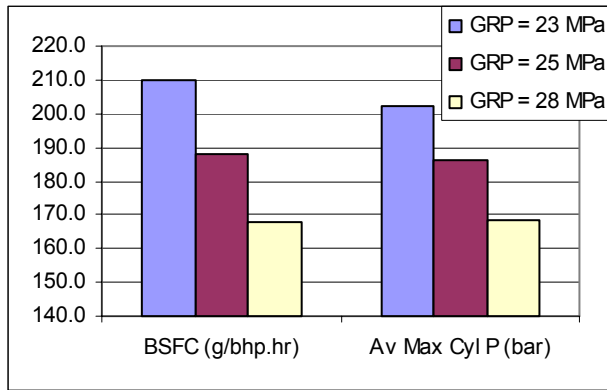


Figure 35: AVL Mode 8 GRP Swings—BSFC and maximum cylinder pressure (Pmax).

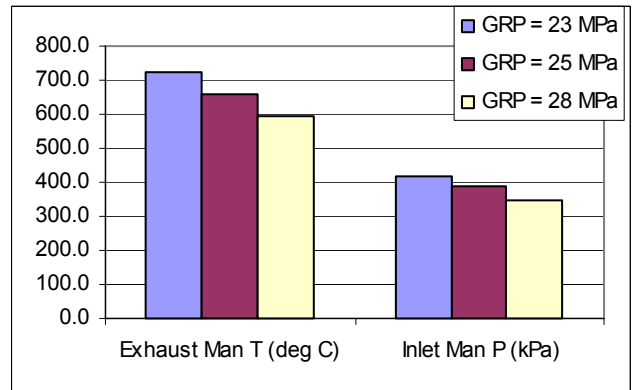


Figure 36: AVL Mode 8 GRP Swings—EMT and IMP

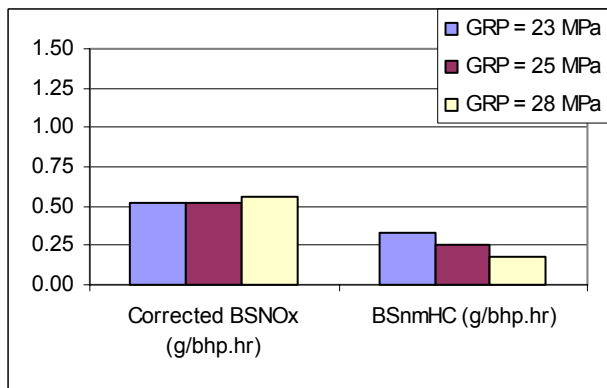


Figure 37: AVL Mode 8 GRP Swings—BSNO_x and BSNMHC

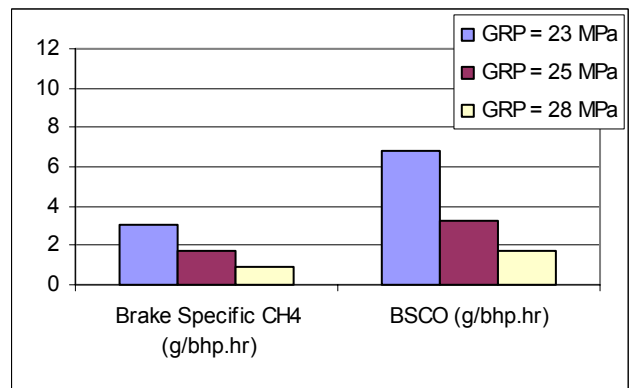


Figure 38: AVL Mode 8 GRP Swings—BSCH₄ and BSCO

The results of the gas pressure swings at ESC mode 10 are shown in Figure 39 through Figure 42. At these high load and speed conditions, high injection pressures give better efficiency. At AVL mode 8, BSFC dropped by about 20% as GRP increased from 23 to 28 MPa. At ESC mode 10, BSFC dropped by about 8.5%. NO_x increased slightly but remained within reasonable limits. Further optimization is expected to reduce these NO_x levels. The higher injection pressures also resulted in reduced emissions of all other regulated pollutants.

